


Ministry of Higher Education and Scientific Research

Kasdi Merbah Ouargla University

Faculty of New Information and Communication Technologies

Dissertation

ACADEMIC MASTER

Domain: Sciences and Technologies

Branch: Telecommunications

Speciality "Systems of telecommunications"

Miniaturization and circularly polarized RFID tag/reader antenna for UHF/SHF band use

Presented publicly by

Bekkoucha Salsabil and Limam Aridj

June 2, 2025

Jury

Mohammed Boulesbaa,	Professor at university of Ouargla	President
Boualem Mekimah,	MCA at university of Ouargla	Supervisor
Amira Hamidi,	PHD at university of Ouargla	Co-Supervisor
Abdelkrim Belhedri,	MCB at university of Ouargla,	Examiner

P
F
E

Dedications

First and foremost, I sincerely thank ''ALLAH'' for the endless mercy, love, and strength that carried me on every step of my journey. God's presence gave me the power to keep pushing forward even when the path seemed impossible.

To the women who believed in me before I believed in myself, my precious mother, your love, encouragement, and prayer shaped me into who I am today. I dedicate this work to you.

To my first hero, my dear father, whom I thank enormously for giving me everything I asked for and more, with love and sacrifice. This achievement is a reflection of your endless support.

To my brother Yacine, the source of wisdom and safety. Thank you for your constant patience and for teaching me since I was a child. Your support means the world to me.

To my dear brothers, Alla and Aymen, even though distance separates us, your love, advice, and support have always been close by. Thank you for being there, no matter how far apart we are.

To my dear sister Tasnim, you were the light of my path, and the safe place that I ran to. Thank you for being the sister who understands without words and supports without asking.

To my best friends: Baraa, Sabrina, and Marina.

To my classmate and friend Aridj.

To all my teachers without exception.

In memory of the innocent lives lost in Gaza, may their pain never be forgotten, and may justice and peace one day prevail. May this humble dedication tribute to resilience, humanity, and hope.

Finally, this success is not my own, it belongs to everyone who stood by me with kindness and faith-Thank you.

BEKKOUCHA Salsabil.

Dedications

Thank God that gave us strength and patience to move forward in our scientific career, which led us to the path of science and knowledge, and helped us complete this work. I dedicate this achievement and important moment of my life with all my heart to:

To my dear mom,

Your love, unwavering support, and sacrifices have allowed me to reach this stage in my academic journey. You've always believed in me, even during moments of doubt. This degree is the result of your encouragements and your constant presence. Thank you for being the strength that has guided me to this point.

To my dear sister Isra,

Your support, your smile, and your kind and encouraging words have always been a source of inspiration and a driving force behind my success May Allah bless you and grant you success in every step you take.

To my dear brothers Amin, Abd Elkader, Issam, Slimane and Isslam,

This achievement is for both of you. Your love, support, and strength have carried me through every challenge. I'm deeply grateful to have you by my side.

To my beautiful grandmother who passed away: Tourkia.

To Manal and Khadidja.

To my classmate and friend Salsabil.

To my teachers thank you for your guidance and wisdom. May God reward you greatly for all you've given me.

Finally deepest thanks to everyone who supported me in this journey.

LIMAM ARIDJ

Acknowledgements

First of all, we would like to thank 'ALLAH' for giving us the strength, power, and faith to finish this work and our journey successfully.

We express our sincere gratitude to our respected supervisor, Dr. Boualem Mekimah, MCA at the University of Ouargla, for his continuous guidance, support, and belief in our abilities. We are truly thankful for the opportunity to be part of his team, for the insightful feedback, and for providing a positive and productive working environment. It has been an honor to work with you.

We would also like to extend our heartfelt thanks to our co-supervisor Mrs. Amira Hamidi, PHD, at university of Ouargla, for her valuable advice, encouragement, and love throughout this work. Her constructive criticism, expertise, and consistent availability were instrumental in helping us overcome challenges and enhance the quality of our project. We are truly gratful for all that.

We would also like to thank Pr. Mohammed BOULESBAA, professor at university of Ouargla, for his sincere interest in our work and for granting us the distinguished honor of presiding over the jury for our graduation project with his deep acquaintance.

We would also like to express our deep gratitude to our examiner in the jury member Dr.Abdelkrim BELHEDRI, MCB at university of Ouargla, for his interest in our work and his willingness to examine and judge it with his constructive questions and experience.

We would also like to express our heartfelt gratitude to all the teachers and professors of the Department of Electronics and Telecommunications at Kasdi Merbah Ouargla University (UKMO) for their dedication, valuable teaching, and unwavering support. We are especially thankful for their patience, guidance, and above all, their humility, which has deeply inspired us throughout our academic journey.

Finally, we would like to thank our families, friends, and all those who contributed to the successful completion of this work, in one way or another.

Abstract

In this work, two antenna designs are proposed. First, we propose a tag antenna which implemented on a square Rogers RO4003C substrate with a compact size of 35 × 35 × 0.508 mm^3. Four triangle shapes are slightly curved that used to enhance the axial ratio and improve circular polarization (CP). The meander lines remained unchanged, but the end circles are replaced with squares to reduce simulation time. Square delay elements with slight curves are also introduced, while the T-match structure was retained for better impedance matching. These modifications aim to adjust the antenna to the UHF band and enhance circular polarization. At the resonant frequency of 915 MHz, the antenna achieves a low reflection coefficient of −31.12 dB. Additionally, a high gain of 1.62 dBic supports a large reading range of 8.84 m in broadside bidirectional radiation, making it highly suitable for long-range RFID applications in random mobility scenarios.

The second part contains a reader antenna which is printed on the RO4003C substrate with dimensions of 104 × 104 × 1.524 mm^3. Two pairs of double-sided dipoles are printed on the top and bottom of the substrate and fed by a 50 Ω coaxial cable. The reader antenna operates using the sequential phase mechanism with phase shifts of 0°, 90°, 180°, and 270° to achieve circular polarization. The dipoles are connected through a concentric ring delay-line feed structure, enabling circular polarization across both frequency bands. The longer and shorter dipoles enable circular polarization in the UHF/SHF bands, providing gains of 1.73 dBi and 5.7 dBi, respectively. At the resonant frequencies of 915 MHz (UHF) and 2.4 GHz (SHF), the antenna achieves low reflection coefficients of −30.87 dB and −45 dB, indicating excellent impedance matching. These features make it well-suited for universal RFID systems operating in the UHF and SHF bands.

Keywords–RFID, Tag antenna, Reader antenna, UHF/SHF band, Miniaturization, Circularly polarized antenna, Impedance matching, T-match.

Résumé

Dans ce travail deux structures d'antennes sont proposées. La première est une antenne étiquette réalisée sur un substrat carré de type RO4003C avec des dimensions compactes de $35 \times 35 \times 0.508\ mm^3$. Quatre triangles ont été légèrement courbés afin d'améliorer le rapport axial et ainsi la polarisation circulaire (CP). Les lignes en méandre sont restées inchangées, mais les cercles aux extrémités ont été remplacés par des carrés afin de réduire le temps de simulation. Des éléments de retard carrés avec une légère courbure ont également été introduits, tandis que la structure en T a été conservée pour un meilleur appariement d'impédance. Ces modifications visent à ajuster l'antenne à la bande UHF et à améliorer la polarisation circulaire. À la fréquence de résonance de 915 MHz, l'antenne atteint un faible coefficient de réflexion de −31.12 dB. De plus, un gain élevé de 1.62 dBic permet une grande portée de lecture de 8.84 m avec un rayonnement bidirectionnel en broadside, ce qui la rend particulièrement adaptée aux applications RFID à longue portée dans des scénarios de mobilité aléatoire.

La deuxième structure est une antenne lecture imprimée sur un substrat RO4003C avec des dimensions de $104 \times 104 \times 1.524\ mm^3$. Deux paires de dipôles double face sont imprimées sur les faces supérieure et inférieure du substrat et alimentées par un câble coaxial de 50 Ω. L'antenne lecture fonctionne selon le mécanisme de phase séquentielle avec des déphasages de0°, 90°, 180°, et 270° pour obtenir une polarisation circulaire. Les dipôles sont reliés par une structure d'alimentation à ligne de retard annulaire concentrique, permettant une polarisation circulaire dans les deux bandes de fréquence. Les dipôles longs et courts permettent une polarisation circulaire dans les bandes UHF et SHF, avec des gains respectifs de 1.73 dBi et 5.7 dBi. Aux fréquences de résonance de 915 MHz (UHF) et 2.4 GHz (SHF). L'antenne affiche de faibles coefficients de réflexion de −30.87 dB et −45 dB, indiquant un excellent appariement d'impédance. Ces caractéristiques la rendent bien adaptée aux systèmes RFID universels fonctionnant dans les bandes UHF et SHF.

Mots clés– RFID, Antenne étiquette, Antenne lecteur, bande (UHF/SHF), Polarisation circulaire (CP), Adaptation d'impédance, T-match.

ملخص

تشهد تقنية تحديد الهوية باستخدام الترددات الراديوية RFID نموًا سريعًا في العالم اليوم، خصوصًا في مجالات مثل الرعاية الصحية، والتحكم في الوصول، وتحديد المواقع. يُعدّ التصغير والاستقطاب الدائري من الجوانب الأساسية في تصميم الهوائيات لكل من الوسم *tag* والقارئ *reader* في هذا العمل.

تم تنفيذ الوسم المقترح على ركيزة مربعة من نوع R*ogers*4003C بحجم مضغوط يبلغ $35 \times 35 \times 0.508\ mm^3$. بالإضافة إلى ذلك، تم تعديل أشكال المثلثات الأربعة بانحناءات طفيفة لتحسين نسبة المحور وتعزيز الاستقطاب الدائري CP . لم تتغير الخطوط المتعرجة *meanderlines* ، ولكن تم استبدال الدوائر النهائية بمربعات لتقليل وقت المحاكاة. كما أُضيفت عناصر تأخير مربعة الشكل بانحناءات طفيفة، وتم الإبقاء على هيكل التوصيل T − *match* لضمان تحسين التوافق المعاوقي. تهدف هذه التعديلات إلى ضبط الهوائي للعمل ضمن نطاق UHF وتحسين الاستقطاب الدائري. عند تردد الرنين 915 ميغاهرتز، يحقق الهوائي معامل انعكاس منخفض قدره 31.12− ديسيبيل. بالإضافة إلى ذلك، يوفر كسبًا عاليًا قدره 1.62 ديسيبل ديوتروني *dBic* ومدى قراءة يصل إلى 8.84 مترًا في إشعاع ثنائي الاتجاه على مستوى السطح، مما يجعله مناسبًا جدًا لتطبيقات RFID بعيدة المدى في حالات الحركة العشوائية.

يتم طباعة هوائي القارئ على ركيزة من نوع R*ogers*RO4003C بأبعاد $104 \times 104 \times 1.524\ mm^3$. وتتم طباعة زوجين من الهوائيات ثنائية الجوانب على الجزء العلوي والسفلي من الركيزة ويتم تغذيتها بكابل متحد المحور بقيمة 50 Ω . يعمل هوائي القارئ باستخدام آلية الطور المتسلسل بتغييرات في الطور مقدارها 0° ، 90° ، 180° ، و 270°

لتحقيق الاستقطاب الدائري. يتم توصيل الهوائيات من خلال هيكل تغذية بحلقة متحدة المركز مع خط تأخير، مما يُمكّن الاستقطاب الدائري عبر النطاقين الترددين. يُمكّن الهوائي الطويل والقصير الاستقطاب الدائري في نطاقي UHF و SHF ، ويوفران كسبًا قدره 1.73 ديسيبل و 5.7 ديسيبل على التوالي. عند ترددات الرنين 0.915 غيغاهرتز UHF و 2.45 غيغاهرتز SHF ، يحقق الهوائي معاملات انعكاس منخفضة بقيم 30.87− ديسيبيل و 45− ديسيبيل، مما يشير إلى توافق معاوقي ممتاز. تجعل هذه الخصائص الهوائي مناسبًا جدًا لأنظمة RFID العالمية العاملة في نطاقي UHF و SHF .

الكلمات المفتاحية RFID ، هوائي العلامة، هوائي القارئ، نطاق UHF/SHF ، هوائي مستقطب دائريًا، T − *match* .

Contents

List of Figures

List of Tables

List of Acronyms and Abreviations

FBW	Fractional Bandwidth
CST	Computer Simulation Technology
EM	Electromagnetic
EPC Gen 2	Electronic Product Code Generation 2
ERP	Effective Radiated Power
ERIP	Equivalent Isotropically Radiated Power
ETSI	European Télécommunication Standards Institute
FCC	Federal Communication Commission
HF	High Frequency
ID	Identification
ISM	Industrial Scientific Medical
ISO	Organization International de Normalization
LBT	Listen Before Talk
LF	Low Frequency
LHCP	Left Handed Circular Polarization
AR	Axial ratio
RF	Radio Frequency
RFID	Radio Frequency Identification
RHCP	Right Handed Circular Polarization
SHF	Super High Frequency
UHF	Ultra High Frequency
VSWR	Voltage Standing Wave Ratio

List of Symbols

f_c	Central frequency
f_1	Lower frequency
f_2	Higher frequency
Z_C	Characteristic impedance
Z_{Ant}	Antenna impedance
R_{Ant}	Antenna resistance
X_{Ant}	Antenna reactance
R_{loss}	Loss resistance
$\Gamma(x)$	The reflection coefficient on a line
s_{11}	The reflection coefficient at the entrance to the antenna
ε	Dielectric permittivity
ε_r	Relative dielectric permittivity
$\tan\delta$	loss tangent
Δ f	Bandwidth
η	Radiation efficiency
$F(\theta,\varphi)$	Radiation characteristic function
$P(\theta,\varphi)$	Power in the direction(θ,φ)
$P(\theta_0,\varphi_0)$	Power in direction of maximum radiation
$D(\theta,\varphi)$	Directionality in direction (θ,φ)
$G(\theta,\varphi)$	Gain in direction (θ,φ)
P_t	Input power
P_r	Power at reception
G_t	Gain the transmitting antenna
G_r	Gain of receiving antenna
E	The electric field vector
E_x	The component of the electric field vector in the x direction
E_y	The component of the electric field vector in the y direction
H_x	The component of the magnetic field vector in the x direction
H_y	The component of the magnetic field vector in the y direction
f	The frequency in Hertz
ω	The pulsation in radians per second, equal to $2\pi f$
k	The wave number in radians per meter
φ_x	The initial phase of the E_x component
φ_y	The initial phase of the E_y component
τ	Transmission coefficient
G_t	Gain of the transmitting antenna

G_r	Gain of the receiving antenna
G	Gain
D	Directivity
Z_{Chip}	Chip impedance
R_{rad}	Antenna radiation resistance
λ	Wavelength

General Introduction

Radio Frequency Identification (RFID) is an emerging technology that is expected to become ubiquitous soon. It allows for the identification of objects by exchanging data through radio frequency signals, such as traceability, medical monitoring of a patient's condition, and production management. In essence, RFID systems are little transponders, or tags, that are affixed to actual objects. They might end up being the most popular chip ever. RFID tags wirelessly respond to RFID transceivers or readers by providing specific identifying information that can be connected to arbitrary data records [1]. RFID systems can be classified according to how frequently they operate and which components they contain. It falls into the low frequency (LF), high frequency (HF), ultra high frequency (UHF) and microwave range for two Industrial Scientific Medical bands (ISM), 2.4 GHz and 5.8 GHz, based on frequency bands [2].

Single-band, large size, low reading range, and polarization losses are the main problems with RFID readers and tags in the literature. We proposed a miniaturized, circularly polarized RFID system consisting of a dual-band reader antenna and a tag antenna with enhanced gain, designed to overcome some of the aforementioned limitations. To help with the creation of the suggested antenna and make it acceptable for a range of RFID applications, we employed the CST Studio Microwave Simulator. The performance of the proposed tag antenna will be evaluated and compared with existing designs reported in the literature, particularly in terms of size, frequency bandwidth, field polarization, gain, and reading range [3–7]. In terms of gain, the proposed tag antenna demonstrates competitive performance compared to works in [3–6]. The work in [7] achieves a high gain of 6 dBi. However, this comes at the cost of occupying a significantly larger surface area of $220 \times 30 \times 1\ mm^3$, as well as, a linearly polarized radiation is shown which makes losses due to the polarization mismatch. It also exhibits a reading range of only 5 meters, limiting its effectiveness in dynamic RFID environments. The proposed tag antenna exhibits an extended reading range in compact size, outperforming several existing designs, which makes it highly suitable for long-range RFID applications. In addition, it provides circularly polarized radiation in a broadside bidirectional radiation, enhancing its reliability in environments with varying tag orientations. In summary, the proposed RFID tag antenna combines compact size, wide operational bandwidth, and improved radiation characteristics, positioning it as a strong candidate for UHF RFID applications involving random mobility scenarios.

As a second part of our work, a circularly polarized RFID reader antenna operating in a dual-band configuration is designed to support both the UHF and SHF frequency bands. This reader antenna demonstrates favorable characteristics, including broad frequency coverage and robust polarization performance, ensuring its suitability for a wide range of RFID systems and promoting universal applicability.

Most previously reported RFID reader antennas are limited in terms of frequency coverage, polarization diversity, and overall adaptability to various RFID systems [8–11]. To this end, we propose a dual-band, circularly polarized RFID reader antenna designed to operate efficiently not only within the UHF and SHF frequency bands but also beyond. Compared to existing reader designs, the proposed antenna offers a broad operational bandwidth and supports circular polarization, enhancing its suitability for universal RFID applications. The antenna enables reliable tag detection regardless of tag orientation or movement, which is essential for ensuring robust performance in real-world, dynamic environments. Moreover, the wide-band capability increases the system's versatility by allowing communication with various types of RFID tags operating over different frequency ranges. In terms of performance, the proposed reader antenna demonstrates stable radi-

ation characteristics, compact size, and high efficiency across the operating frequency bands. These features make it an ideal candidate for advanced RFID systems that require robust, wide band, and polarization-agile reader antennas.

The current manuscript is organized as follows:

The first chapter presents a comprehensive overview of RFID technology, with a focus on its fundamental components, including readers, tags, and data processing systems. It begins by detailing the working principles of RFID, followed by a classification of different types of RFID tags. The chapter also outlines relevant standards, regulations, and common coupling techniques used in RFID systems. Special emphasis is placed on passive UHF RFID systems, highlighting their structure and wide range of applications. The chapter concludes with a critical analysis of the advantages and limitations of RFID technology, offering a well-rounded understanding of its capabilities and practical implications.

The second chapter begins with a review of fundamental antenna characteristics, with particular emphasis on patch antennas due to their relevance in RFID applications. It then explores various feeding techniques used for patch antennas, which significantly influence their bandwidth, impedance matching, and radiation performance. Additionally, the chapter introduces the meandering strategy employed in antenna miniaturization and design, followed by a discussion on impedance-matched antennas. These topics collectively aim to build a solid foundation for understanding the key aspects of antenna design and performance.

The third chapter is dedicated to the design and simulation of a dual-band, circularly polarized (CP) RFID reader antenna capable of operating across both UHF and SHF frequency bands, 0.915 GHz and 2.45 GHz. The antenna's key characteristics—including axial ratio, return loss, realized gain, efficiency, and radiation pattern—are presented and analyzed. All simulations and performance evaluations are carried out using CST Studio Microwave Software, ensuring accurate modeling and validation of the proposed design.

The fourth chapter focuses on the design and simulation of a miniaturized, circularly polarized RFID tag antenna operating in the UHF band at 915 MHz. The chapter presents a detailed analysis of the antenna's performance, including axial ratio, return loss, realized gain, efficiency, and radiation pattern. All simulation results are obtained using CST Studio Microwave Software, ensuring accurate and reliable performance evaluation of the proposed design.

The manuscript concludes with a general conclusion that highlights the key outcomes of this work, emphasizing the main contributions and potential applications of the proposed RFID system.

Chapter 1

Radio-frequency identification systems

Sommaire

1.1 Introduction

RFID (Radio-frequency Identification) technology is a wireless communication technology used to capture data, which may be linked to different identification attributes (serial number, position, color, date of purchase, etc.) of entities carrying RFID labels (tags). The data collection process is based on an exchange of electromagnetic waves between RFID tags and RFID readers. This Automatic Identification and Data Capture (Auto-ID) technology is capable of providing further labelling granularity when compared to barcodes and previous Auto-ID technologies. For instance, with RFID, it is possible to allocate different identification codes for similar items, and different levels of identification allowing better visibility and tractability in logistical and manufacturing processes [12]. The first chapter is structured as follows: first we will present a few concepts of RFID systems, the various components of RFID, such as readers, tags, and data processing systems, the working principle will be outlined, and we will examine many types of tags, rules, and guidelines of RFID technology and the types of couplings. In addition, we will discover passive UHF RFID systems and several RFID applications. Finally, we will examine the benefits and limitations of RFID technology.

1.2 RFID systems

RFID or Radio Frequency Identification is a wireless communication system that uses modulated backscattered waves to provide the radio link between the base station and the transponders. An RFID system is composed of three main elements: The RFID tag, which contains an electronic chip and an antenna, the chip stores information that can be read remotely. The RFID reader emits radio waves to interrogate nearby tags. Then, the data processing system collects and analyzes the information transmitted by the reader as shown in figure 1.1 [13, 14].

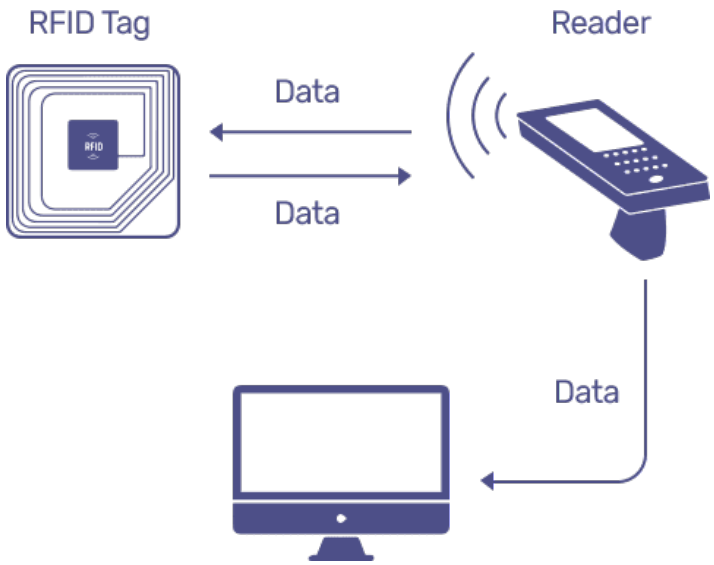

Figure 1.1: RFID setup.

1.3 RFID Components

An RFID system operates by transmitting and receiving an electromagnetic signal via an antenna and an integrated circuit (IC) [15]. An RFID system consists of two components :

- The transponder, which is located on the object to be identified.
- The interrogator or reader, which depending on the design and technology used, may be a read-only or read/write device [16].

1.4 RFID reader

RFID readers use a radio frequency (RF) channel to communicate with RFID tags and gather identifying information. RFID readers usually have two interfaces to extract tag identities: an RF interface to interact with tags within their read range and a communication interface, usually IEEE 802.11 or 802.3, to establish a connection to servers [17]. There are two types of RFID readers: fixed and mobile.

1.4.1 Mobile reader

Mobile readers or handheld readers. These devices typically do not have additional antenna connectors because they come with an integrated antenna. They weigh between 82 and 700 grames, run on batteries, and have reading ranges of only 100 meters, which is less than stationary readers. Mobile readers are commonly used to locate products in inventory and warehouses, track livestock (farm animals such as sheep, goats, and cows), and more. They use wireless communication protocols to connect with a PC host, which stores data in the memory block. Since handheld RFID readers are often combined with barcode scanner, users may identify tags and barcodes using a single device, opening up a wide range of versatile applications [14].

Figure 1.2: Mobile RFID reader.

1.4.2 Fixed RFID Reader

Stationary readers, also known as fixed RFID readers figure 1.3, are designed to be installed in a permanent location, such as walls, gates, doors, or other objects, where they

can perform efficient tag readings. These readers are mainly used in wireless data collection applications, like in supply chain management and asset and product control. These days, fixed RFID readers mounted on gates and doors are utilized for both personnel identification and authentication in restricted-access zones. They can provide reading ranges of up to 300 meters and weigh between 1.5 and 5 kg [14].

Figure 1.3: Fixed reader.

1.5 RFID Tag

RFID tag or transponder is a small electrical device used to store and transmit data and information wirelessly using radio frequency signals. It consists of: an antenna, a basic silicon microchip, and a chip-based data collection system. The tag can be fastened to an item such as, a box, clothes, and other objects with several different formats as shown in figure 1.4 [18].

Figure 1.4: Different forms of tag.

1.5.1 Types of RFID Tags

A wide range of RFID tag types are available, where each tag is designed with specific features and applications. Choosing the right tag type allows operations to be optimized

and better based on factors such as range, environment, and cost.

1.5.1.1 Active RFID tags

The tag's built-in battery can supply the processor with the energy it needs to generate the signal. Because the reader does not need to power the tag, it only needs to provide very low-level signals to it. As a result, the active tag can read far farther than the other two tags, and its chip can access memory more readily. An active tag's primary advantage is its ability to actively communicate with the reader by using its own power source. Furthermore, whether or not an RFID tag is in the reader's field, it is always powered on. Despite having the best capabilities, this form of tag has a battery life limit and stops working when the battery runs out, unlike the other two varieties. Active tags are typically big and costly to make because of the integrated power supply [19]. Active RFID tags are capable of transmitting signals within frequency ranges of 433 MHz to 2.45 GHz. Typically, active beacons and transponders have a lifespan of 3 to 5 years without requiring a battery replacement, if permissible. Additionally, active RFID tags can achieve a communication range exceeding 100 meters.

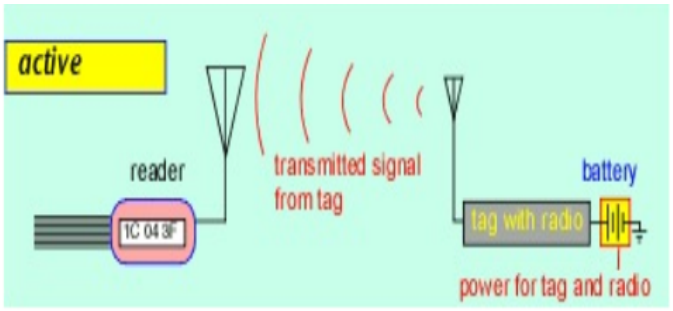

Figure 1.5: Schema representation of Active Tag.

1.5.1.2 Passive RFID Tag

A passive UHF RFID tag consists of a chip and an antenna. It is called passive because it does not have its own energy source. It is remotely powered by transforming the electromagnetic energy radiated by the reader hwo transmit data into continuous electrical energy necessary for the activation and operation of its chip [20]. They function within a frequency range of 125 KHz (LF) to 960 MHz (UHF). Their lack of moving parts or internal power sources contributes to their longevity. The maximum reading distance for passive RFID tags can reach up to 15 meters, while the minimum range is between 1 to 10 centimeters.

1.5.1.3 Semi-passive RFID Tag

Semi-passive tags and passive tags are extremely similar, however they differ in that the former have a battery that powers the chip exclusively, as seen in Figure. These tags were created with the intention of preserving the reader's energy output, particularly when it is poor, and preventing the chip from being powered by it. This explains why semi-passive tags function effectively even in the presence of a weak signal. Semi-passive tags perform better in terms of reading distance and communication quality with the reader [21].

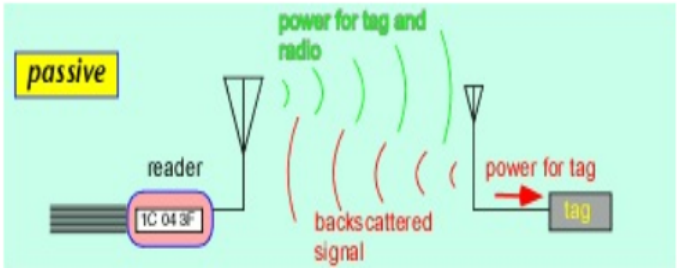

Figure 1.6: Schema representation of passive tag.

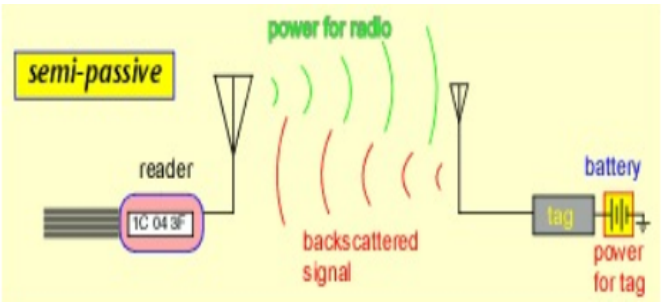

Figure 1.7: Schema representation of semi-passive tag.

1.6 Operating principle of RFID systems

Three parts make up every RFID system: a transceiver, a transponder, and a scanning antenna. An RFID reader or interrogator is the term used to describe the combination of the transceiver and the scanning antenna. RFID readers come in two varieties: mobile readers and fixed readers. RFID reader is a network-enabled gadget that can be fixed or carried about. It transmits impulses that activate the tag via radio waves. When the tag is engaged, it transmits a wave back to the antenna, which converts it into information. RFID tag itself contains the transponder. The type of tag, reader type, RFID frequency, and interference from other RFID tags and readers or the surrounding environment all affect the reading range of RFID tags. The reading range of tags with a more powerful power source is also longer.

1.7 Operating frequency and reading range for RFID systems

Between the electrical and infrared signals is the radio frequency signal. It has a broad frequency range of 3 KHz to 300 GHz. Systems that use radio frequency identification (RFID) are often categorized according to their operating frequency spectrum. The length of radio waves utilized for system component communication is indicated by frequency. The low frequency (LF), high frequency (HF), ultra-high frequency (UHF), and super-high frequency (SHF) bands are used by RFID technology worldwide. Every frequency band has its own operational range, power needs, performance, and range of applications, and radio waves behave differently in each of these bands. The previous bands are shown in figure 1.8 [1].

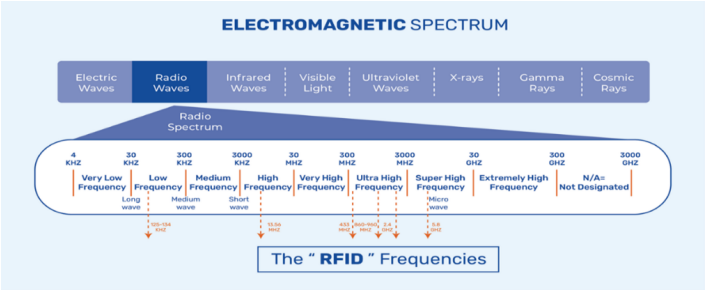

Figure 1.8: Operating frequency and reading range for RFID systems.

1.7.1 Low frequency (LF) band

The frequency range covered by the LF band is 30 KHz to 300 KHz. Although RFID LF systems typically operate at 125 KHz, some operate at 134 KHz. This range of frequencies provides a brief range of approximately 10 cm. While its reading speed is slower than that of higher frequencies, it is not particularly sensitive to radio interference. Applications for RFID LF include access control and detailed tracking [1].

1.7.2 High frequency (HF) band

The 13.56 MHz is the frequency at which high-frequency (HF) RFID tags function. HF tags are frequently presented in a credit card form factor or foil inlay. Thus, HF tags are helpful for ID badges, contactless payment cards, and building access control. Several asset-tracking applications also make use of HF tags. HF foil inlays are frequently used by retailers and libraries to trace books. HF RFID luggage tags are now being used in several airports for baggage handling purposes. Although HF tags have a faster data read rate than LF tags, they are less effective when placed close to liquids or metals [1].

1.7.3 Ultra high frequency (UHF) band

The range of frequencies covered by the UHF band is 300 MHz to 3 GHz. Despite regional variations in frequency, RFID RAIN systems typically operate between 900 and 915 MHz in most countries. The reading range of passive UHF systems can reach 12 meters, and RFID UHF has a faster data transfer rate than LF or HF. Although UHF RFID technology is the most sensitive to interference, many UHF product manufacturers have managed to design tags, antennas, and readers that maintain high performance even in challenging environments. Compared to LF and HF, UHF passive labels are easier and less complicated to manufacture. Long-range RFID systems are those that have ranges much greater than one meter. All long-range systems use microwave and UHF electromagnetic waves to function. Because of their physical working principle, the majority of these systems are also referred to as backscatter systems. Furthermore, there are long-range systems that use microwave-range surface acoustic wave transponders. All of these systems run on the microwave frequencies of 2.5 GHz and 5.8 GHz as well as the UHF frequencies of 868 MHz (Europe) and 915 MHz (USA) [16].

1.7.4 Super high frequency (SHF) band

Super high frequency (SHF) band operates in the 2.45 GHz and 5.8 GHz range and use radiative coupling for communication. A transponder's passive SHF range can reach up to three meters, a distance that can reach 300 meters if you choose to use active transponders. The rate of RFID SHF system transfers is extremely high among all RFID frequency bands, enabling rapid and efficient data exchange. SHF signals are easily affected by moisture and metals, and they have limited ability to penetrate obstacles. In addition, SHF RFID systems are typically more expensive and require complex infrastructure, making them more suitable for specialized applications such as electronic toll collection, transportation monitoring, and high-speed asset tracking. The following table displays the differences and features of the previous bands, table 1.1 [22].

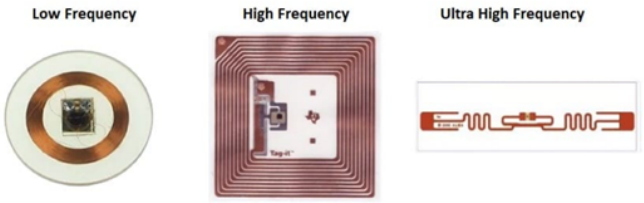

Figure 1.9: Some examples of LF, HF, and UHF tag antennas.

Table 1.1: Comparison of radio frequency ranges and characteristics of different RFID systems [22].

Description	**Low Frequency**	**High Frequency**	**Ultra-high Frequency**	**Super-high Frequency**
Frequency range	125–134 KHz	13.56 MHz	850–950 MHz	2.45 or 5.8 GHz
Coupling	Inductive	Inductive	Radiative	Radiative
Tag type	Passive	Passive	Active/Passive	Active/Passive
Read range	0–0.5 m	<1.5 m	Active: 3–10 m, Passive: >10 m	Active: 3–10 m, Passive: >10 m
Tag size	Larger	Larger	Smaller	Smaller
Data transfer rate	Slow	Medium	Fast	Fastest
Ability to read near metal or wet surface	Best	Better	Worse	Worst
Tag cost	High	Higher than LF tags	Lowest	High
Typical applications	- Livestock tracking - Beer kegs - Auto keys and locks - Library books	- Item-level tracking - Airline baggage - Building access	- Supply chain tracking - Warehouse management - Case, pallet, truck, trailer tracking	- Electronic toll collection - Railroad monitoring
Advantages	- Works well near liquids and metals - Global standards - No radiation/reflection problems	- Larger memory - Global standards - Tolerant to fluids/metals	- Long read range - Write large amounts of data - Low-cost readers - High data rate	- Long read range - High commercial potential
Disadvantages	- Very short read range - Limited memory - Low transmission rate - High cost - Not ideal for warehouses	- Higher read rate than LF - Still low transmission rate - Poor metal compatibility	- High tag cost - Requires complex software - Ineffective in moist environments	- Most expensive - Complex system development

1.8 Coupling types in RFID systems

The crucial differentiation criterion for RFID systems is the physical coupling method. The two main types of RFID systems currently available for purchase are far-field systems, which are coupled with real free-space energy that emits planar electromagnetic waves, and near-field systems, which use inductive (magnetic) tag coupling with RF reactive energy circling the reader's antenna. Electric, magnetic and electromagnetic fields are used for the physical coupling. In addition, RFID systems with a narrow range, typically in the region of up to 1cm, are known as close coupling systems. Close-coupling systems are coupled using both electric and magnetic fields and can theoretically be operated at any desired frequency between DC and 30 MHz because the operation of the transponder does not rely upon the radiation of fields [16].

1.8.1 Magnetic (inductive) coupling

Near field systems or inductive coupling, a single microchip, large-area coil, or conductor loop serving as an antenna make up an inductively coupled transponder. Since these transponders are usually passive, the reader must provide the energy required for the microchip to function. The reader's antenna coil creates a strong, high-frequency electromagnetic field that permeates the coil's cross-section and surrounding surroundings. The electromagnetic field functions as a straightforward magnetic alternating field since the frequency's wavelength is significantly larger than the distance between the transponder and the reader's antenna. Only a tiny percentage of this field makes it to the antenna coil of the transponder, which is placed at a distance away from the coil of the reader. After rectification, the voltage produced by the transponder's antenna coil's inductance powers the microchip. Figure 1.10 below illustrates the system.

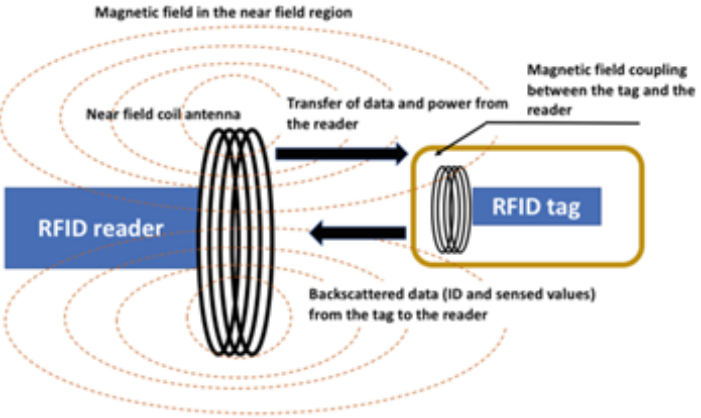

Figure 1.10: Near field system.

1.8.2 Far-field systems

Data sharing in the UHF or SHF range depends on electromagnetic (EM) wave propagation. An electromagnetic wave is produced when a high-frequency signal is applied to the reader antenna. On the other hand, an electrical voltage shows at the tag antenna's terminals when it is positioned in the electromagnetic field that the reader produces. The tag

chip is powered by this voltage. The antennas on passive UHF RFID tags come in a variety of shapes for radiative coupling. The application is the primary determinant of the RFID antenna selection. The antenna's cost, which comprises the substrate, chip-fixing tools, and antenna material (conductive ink, copper, etc.), is the main limitation. The antenna's size, which ultimately dictates the label's size, is the second limitation. For the size, the application should be considered.

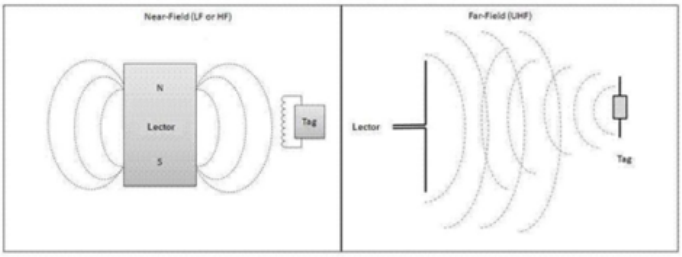

Figure 1.11: Comparison between far field and near field in RFID.

1.9 RFID system interference

1.9.1 Reader/Tag interference

When several concurrent queries from several readers are sent to a tag, this is known as a reader-to-tag collision (tag interference). This problem can be solved by assigning different channels to nearby readers [23]. This may stops the tag from being read when multiple readers attempt to read it at the same time. In practice, when two or more readers attempt to read the same tag, the latter cannot be read if the difference between their signal intensities is greater than the threshold that the tag can withstand. However, by employing a filter that reduces some of the interference, the tag can react to one of the conflicting signals. For a tag to distinguish between two colliding signals and react to a single reader, there must be an intensity differential of 6 to 15 dB (tolerance) [24].

1.9.2 Reader/Reader interference

A reader-to-reader collision occurs when neighboring readers simultaneously interrogate a specific tag in the same frequency band. Furthermore, it may occur when the tag is within the readable range of one reader and the interference range of the other reader; the signal from the latter reader may interfere with the return signal from the tag [25–28]. This can be solved by assigning different channels to neighboring readers [29].

1.9.3 Tag/Tag interference

When several signals reach the reader at once, it is impossible to reliably detect every tag inside its interrogation zone, resulting in a tag-to-tag collision. Figure 1.12 depicts this situation, in which tags T1, T2, T3, and T4 all send signals to the same reader at the same time, making it impossible for the reader to identify a specific tag. The data from these tags would collide at the reader without an anti-collision mechanism, deteriorating their identification and wasting energy and bandwidth [11, 30–32].

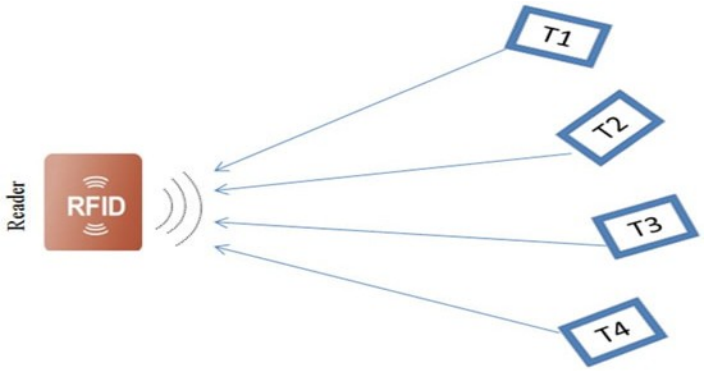

Figure 1.12: Tag-to-tag collision.

1.10 Regulations and standards for RFID systems

1.10.1 Regulations of RFID systems

The selection of operating frequency in RFID systems is determined by the specific application requirements, However, compliance with regulatory standards is essential. These regulations help prevent interference with other radio communication systems. To support global compatibility, certain frequency ranges, termed ISM (Industrial, Scientific, and Medical), have been designated for such use. The frequencies most commonly used in RFID applications are 135 kHz, 13.56 MHz, and 2.45 GHz, corresponding to low, intermediate, and high-frequency bands, respectively [33]. Table 1.2 outlines the key regulatory standards for RFID systems.

1.10.2 Standards of RFID systems

Driven by industry and user demands, the continuous development of standards, particularly testing protocols, is essential to master RFID technology and expand its market reach. These standards certify system interoperability, component interchangeability, and operational reliability. ISO has established key standards that govern parameters such as frequency, bandwidth, power limits, modulation, data rates, and communication protocols. Table 1.3 outlines the key ISO standards.

Table 1.2: UHF RFID spectrum allocations by region [34].

Region	Frequency Range	Authorized Powers
Europe	869.4 to 869.65 MHz 865 to 868 MHz 865.6 to 867.6 MHz 865.6 to 868 MHz	500 mW ERP 100 mW ERP-LBT 2 mW ERP-LBT (10 channels of 200 KHz) 500 mW ERP-LBT
America	902 to 928 MHz	4W EIRP-FHSS (80 channels of 325 KHz)
Asia and Oceania	Japan: 952 to 954 MHz Korea: 908.5 to 914 MHz Australia: 915 to 928 MHz	4W EIRP 4W EIRP 1W EIRP

For passive UHF RFID, ISO-specific standards include:

- **ISO 18000-6**: Communication protocol
- **ISO 18047**: Conformance testing
- **ISO 18046**: Performance evaluation

Currently, the EPCglobal consortium (headed by GS1, which unified EAN and UCC barcode systems) developed the *EPC Class-1 Generation-2* standard to streamline the reader-tag interfaces and promote the adoption of RFID. Unlike ISO, EPCglobal focuses exclusively on traceability applications, with the aim of establishing an Internet of Things framework. Its strength lies in managing both technical specifications and unique tag identification codes leveraging existing barcode standardization infrastructure [16].

Notably, major industry players and research laboratories support EPCglobal, and its UHF identification standards now converge with ISO frameworks.

Table 1.3: Overview of ISO/IEC 18000 RFID Standards by Frequency and Status

Reference	**Frequency**	**Title**	**Status**
18000-1	definitions	RFID for object management – Part 1: Reference architecture and definition of parameters to be standardized	Published on 13/09/2004
18000-2	<135 kHz	RFID for object management – Part 2: Communications parameters of an air interface below 135 kHz	Published on 13/09/2004
18000-3	13.56 MHz	RFID for object management – Part 3: Communications parameters of an air interface at 13.56 MHz	Published on 13/09/2004
18000-4	2.45 GHz	RFID for object management – Part 4: Communications parameters of a 2.45 GHz air interface	Published on 31/10/2004
18000-5	5.8 GHz	RFID for object management – Part 5: Communications parameters of a 5.8 GHz air interface	No consensus
18000-6	860–960 MHz	RFID for object management – Part 6: Communications parameters of an air interface between 860 and 960 MHz	Published on 31/10/2004
18000-7	433 MHz	RFID for object management – Part 7: Communications parameters of a 433 MHz air interface	Published on 12/12/2005

1.10.3 Radio Link Budget in RFID Systems

A typical UHF RFID system consists of a reader and several passive tags. In the uplink communication, the reader interrogates the tag by transmitting data using Amplitude Shift Keying (ASK) modulation. The return communication, from the tag to the reader (downlink), utilizes a backscattered modulation scheme. In the uplink communication, the reader generates a carrier signal, which is radiated through the antenna. The tag collects energy from the electromagnetic waves emitted by the reader and converts it into DC power for the chip. Once powered, the tag is ready to receive commands, which are transmitted by modulating the reader's carrier signal. After completing the command sequence, the reader sends an unmodulated continuous wave (CW) signal to provide continuous DC power for the tag. The power available for the tag's operation (Pr, tag) is determined by a modified version of the Friis transmission equation [35].

1.11 Innovative applications of RFID

1.11.1 RFID technology in the food industry

RFID tags are used in supply chain management to monitor food items while they are distributed and stored. For this specific application, barcode scanners are replaced by RFID technology. Compared to barcodes, RFID technology offers the following benefits: RFID systems can read tags without requiring line of sight, have a wider operating range than barcodes, allow readers to connect with numerous RFID tags at once, and store more data than barcodes [36].

Figure 1.13: RFID chain management and monitoring food.

1.11.2 Patrolling Log Applications

RFID technology is also used to audit and control security personnel themselves. The app provides checkpoints to monitor security guards. Checkpoints are the RFID tags that security guards need to scan during their successive patrols through a reader. The reader keeps a record of the time and point at which the security guards swiped their cards. This will not only help security company management to check the performance of security guards but also serve as a reference to track events. This app can also help to improve the patrol process, for example by identifying the need for increased patrols or checkpoints in the patrol area [37].

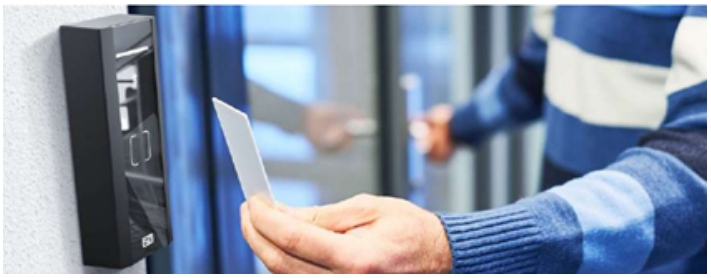

Figure 1.14: RFID access control.

1.11.3 Baggage applications

The airline industry and package delivery services face significant financial losses due to the delay or misplacing of packages and baggage. Managing a diverse range of packages travelling from several locations to different destinations on many paths may be highly complex. In these cases, RFID technology has a significant role to smooth and ease the operation by ensuring efficient package handling. It facilitates package identification and provides detailed records that assist the airline industry in finding areas of improvement, and keep customers informed about their package status [37].

Figure 1.15: RFID technology in airline industry.

1.11.4 RFID applications with animals

Animal identification has been known since ancient times to determine ownership and recover lost or stolen animals. Early methods included tattooing, branding, ear notching and ear tags. Nowadays, electronics and biometric IDs are more common, as shown in Figure 1.16 [38]. In livestock management, RFID technology is commonly used to effectively identify and track individual animals, such as cows and goats. Every animal has a UHF RFID tag, which is usually fixed to its ear and covered in sturdy plastic. Two disks joined by the animal's ear make up the conventional design. During inventory checks, farmers can now swiftly and easily identify their animals thanks to this technology, which significantly improves management effectiveness. Livestock management has

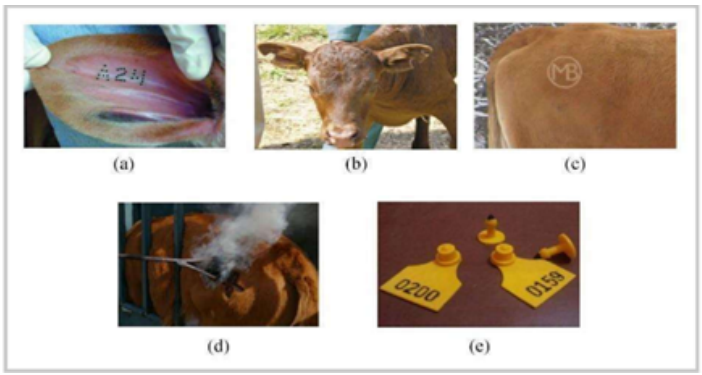

Figure 1.16: Traditional animal identification methods. (a) tattooing (b) ear notch (c) cold stamping (d) hot stamping (d) ear tag.

been transformed by UHF RFID, which provides a more efficient and fruitful method [38].

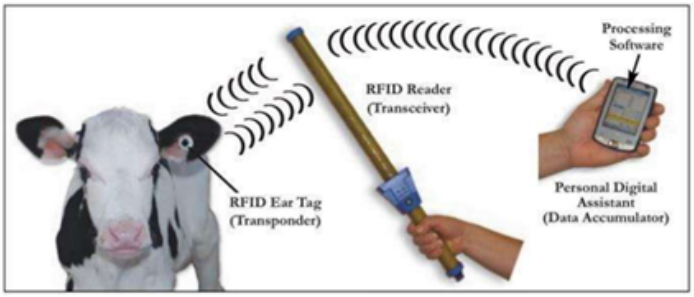

Figure 1.17: Applications of RFID tags.

1.11.5 RFID applications in libraries

RFID uses flexible, thin tags that are placed inside document covers. The Library Management Software has the details of every document as shown in figure 1.18. Without staff help, an RFID reader scans the tag on a document brought in by the user for issuance or return, updating the system in seconds. In order to prevent theft, antennas at the library exit automatically check to see if the document has been issued correctly and sound an alert if it hasn't or is being stolen. In addition to circulation, RFID is utilised in libraries for stock-taking [39].

1.11.6 Automatic toll road applications

RFID applications make toll collection/charging better with improved traffic flow, as cars and vehicles cannot pass through toll stations without stopping for payment. RFID is used to automatically identify the account holder and make faster transactions. This application helps to keep good traffic flow and to identify traffic patterns using data mining techniques that can inform the administration or decision support systems. For example, the information can be used to report traffic conditions or to extend and develop future policies.

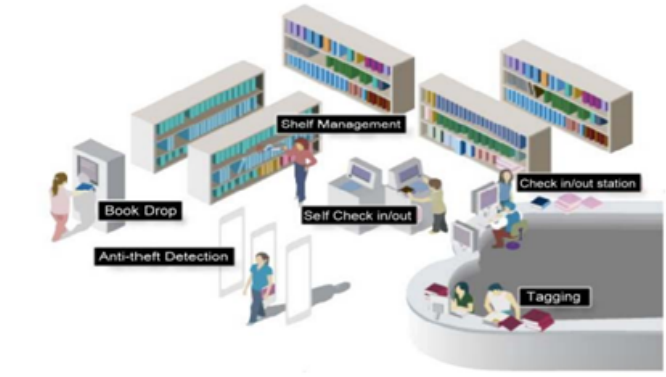

Figure 1.18: Library RFID management systems.

Figure 1.19: Toll road application.

1.11.7 Waste management

Waste management is another area where RFID technology can be applied. Each trash can is fitted with an RFID tag in this system, while garbage trucks are equipped with RFID readers. The reader wirelessly transmits the data to the driver's cabin after scanning the tag on a bin that has been emptied into the truck. The data, which includes the collector's name, collection time, and bin number, is sent to the central server at the end of the route [40].

Figure 1.20: RFID waste management.

1.12 Passive UHF RFID system

In recent years, research has focused on passive UHF RFID technology, which has grown in popularity. This provides a very affordable option. In comparison to other passive RFID technologies, it also provides a greater reading distance (3 to 10 m) and a higher data throughput (about 200 kbit/s). Because of this desire, most parts of the world have adopted laws and industry norms, which has allowed the market for this technology to grow [20]. A passive UHF RFID system, as shown in Figure 1.21, consists of two elements tag and reader [14].

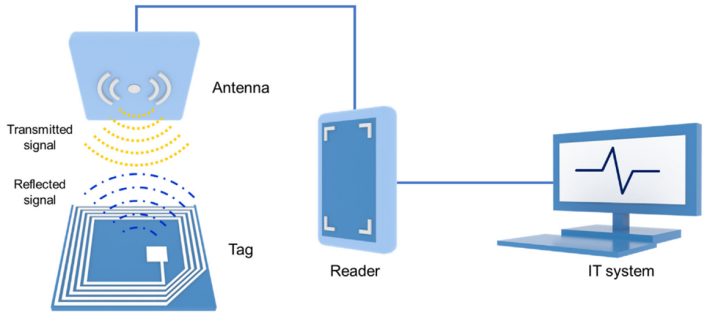

Figure 1.21: Passive UHF RFID system.

1.12.1 Performance criteria in passive UHF RFID communication

A number of traits of both the tag and the reader work in tandem to determine how well RFID communication works. A radiofrequency sinusoidal wave is released by the reader with the dual purposes of powering the tag and facilitating the information transmission (the emitted wave is modified in transmitter mode). The reader's maximum power output is controlled. It is defined by the Equivalent Isotropic Radiated Power (EIRP), which is the result of multiplying the antenna gain (PGr) by the power applied or transmitted to the antenna (Pth). The European Telecommunications Standards Institute (ETSI) sets the maximum EIRP level in Europe, which is equivalent to 3.2W (for the original frequency range); the Federal Communication Commission (FCC) sets the EIRP level in the US, which is worth 4W [41].

1.12.1.1 Transformation of energy and information between tag and reader

A passive UHF RFID tag is composed of an antenna and an integrated circuit. The first function of this circuit is to recover the energy transmitted by the reader in order to provide the power supply necessary for its own operation, and secondly, to ensure its other tasks including the impedance switching at the origin of the transmission of information by retro-modulation from the tag to the reader. Thus, a rectifier converts the alternating current from the reader's RF signal into a direct current providing power to the integrated circuit. The architecture of this rectifier is based on a Cockcroft-Walton type circuit which is composed of two or more stages of diode voltage doublers whose non-linear behavior is at the origin of the harmonics returned by the tag [42]. As a result, in order to activate the tag chip, the RFID reader must send enough power (within the permitted limit) to exceed the tag's minimum activation power (Pth), also known as its sensitivity. After communication is established, the reader (in receiver mode) needs to be able to demodulate

the tag's returned information. As a result, it needs to be able to identify the backscattered signal in general as well as differentiate between the two levels that correspond to the modulation [41].

1.12.1.2 Power transfer between the antenna and the tag chip

The power transfer between the antenna and the RFID tag chip is optimal (i.e., 50% of the power effectively transmitted), and a fundamental condition known as impedance matching in the radio frequency domain is met. This means, the antenna impedance (Z_{ant}) is equal to the complex conjugate of the chip impedance (Z^*_{chip}) in the frequency range [13, 43]:

$$Z_{ant} = Z^*_{chip} \tag{1.1}$$

with

$$Z_{chip} = R_{chip} + jX_{chip} \tag{1.2}$$

$$Z_{ant} = R_{ant} + jX_{ant} \tag{1.3}$$

Thus, the matching conditions become:

$$R_{chip} = R_{ant} \tag{1.4}$$

$$X_{chip} = -X_{ant} \tag{1.5}$$

1.12.1.3 Impedance matching in RFID

Unlike traditional RF systems which commonly used 50 Ω, RFID systems do not follow this standard. Instead, the chip impedance is predefined as specified in manufacturer datasheet, and the matching network is designed accordingly to achieve impedance matching [41].

1.12.1.4 Transmission coefficient

The transmission coefficient, which varies between in the range of 0 to 1, quantifies the efficiency of the impedance matching. It is calculated by:

$$\tau = \frac{4R_{chip}R_{ant}}{\left|Z_{chip} + Z_{ant}\right|^2} \tag{1.6}$$

1.12.1.5 Passive UHF RFID system in the 860-960 MHz and 2.4 GHz bands

Passive UHF RFID system at 860-960 MHz is the most commonly used in RFID applications. This technology offers a higher reading range than 2.4 GHz passive UHF RFID systems, reaching several meters depending on the specifications of RFID tags and readers. Passive UHF RFID tags at 860-960 MHz are often used for supply chain management, logistics, product traceability, asset tracking, access control, etc. Passive UHF RFID readers at 860-960 MHz are available in different sizes and shapes, ranging from handheld to fixed readers, to meet the needs of different applications. This technology is widely used in industry and enterprises to improve operational efficiency and reduce costs [44]. Passive 2.4 GHz RFID systems are used in applications that require very short-range reading,

typically less than one meter. Passive 2.4 GHz RFID tags are often used for in-store inventory management, asset management, retail item tracking, etc. Passive 2.4 GHz RFID readers are available in various sizes and shapes, ranging from handheld to fixed readers, to meet the needs of different applications. Passive 2.4 GHz RFID tags are often less expensive than passive 860-960 MHz UHF RFID tags, making them more economical for short-range reading applications [44]. Although this technology is not suitable for all applications, it is very effective for applications that require short-range reading (inventory management). The choice between 860-960 MHz and 2.4 GHz passive RFID systems depends on the application specifications and read range requirements. The 860-960 MHz passive UHF RFID system offers a higher read range, while the 2.4 GHz passive RFID system is more cost-effective for short-range reading applications.

1.13 Passive UHF RFID systems and their environment

1.13.1 Deployment of passive UHF RFID systems in their environment

The deployment of RFID systems is particularly interesting from the point of view of electromagnetic compatibility. It requires first carrying out a spectral analysis of the site and taking into account interference that may occur between readers [41].

1.13.1.1 Spectral analysis of the environment

Implementation on a site involves carrying out a spectral analysis in order to minimize interference [45]. Indeed, UHF RFID operates in the ISM (Industrial, Scientific and Medical) band, in which many disruptor including GSM can intervene. This measurement makes it possible to identify disruptive sources and to take precautions to minimize their effects on RFID systems.

1.13.2 Passive UHF RFID tags in their environment

Although it is a passive element that does not transmit radiofrequency waves, the design of a passive UHF RFID tag must take into account the constraints related to its environment. First of all, a tag must be operational in a multi-tag environment. It must also be adapted to its immediate environment, and in particular to the object with which it is associated. Finally, it must be immune as much as possible against electrostatic discharges to which it may be subjected.

1.13.2.1 Multi-tag environment

In the identification process, multiple tags may be present in the electromagnetic field of an RFID reader. Collision between tags is generally avoided by two types of approaches, both described in [46]:

• probabilistic approaches based on the ALHOA protocol, which make it possible to reduce the probability of collision by making the tags respond at different time intervals.

• deterministic approaches based on sorting tree protocols. This type of protocol consists of dividing the groups of tags queried into subgroups until all the tags have been identified.

1.13.2.2 Effect of the environment on RFID systems

RFID tags are designed to be associated with objects whose electromagnetic properties are different and influence the properties of the tag (adaptation of the antenna to the chip, etc.). These characteristics must therefore be taken into account from the design of the tags in order to minimize the effects of the environment and optimize the performance [47, 48].

1.14 Benefits of using an RFID system

Although RFID is unlikely to completely replace traditional barcodes in the near future, it provides many advantages that make it valuable for identification purposes such as [49]:

- **Reduces human intervention:** Minimizes human error during data collection and lowers labor costs.
- **Read/Write capabilities:** Unlike barcodes, RFID tags can store and update a greater amount of data.
- **Flexible tag positioning:** No line-of-sight is required, allowing more placement options and less strict alignment.
- **Simultaneous tag reading:** Multiple tags can be scanned at once, which minimizes the time required for circulation operations and provides a much faster alternative to barcodes.
- **Lower inventory costs:** Helps reduce expenses associated with stock management.
- **Durability:** Resistant to dust, chemicals, and physical damage.

1.15 Challenges and limitations of RFID

Challenges and limitations of RFID systems are as follows [49]:

- **Standardization:** Incompatible data formats, communication methods, and collision management result from a lack of consistent standards.
- **Cost:** The economic viability of widespread use is limited by high tag prices, particularly for active and semi-passive tags.
- **Signal collision:** When several tags are read at once, data loss may occur, necessitating the deployment of expensive anti-collision techniques.
- **Frequency issues:** Performance and compatibility are impacted by international frequency regulations, transmission types, and environmental interference (such as water or metals).
- **Tag defects and detection issues:** Read failures may result from manufacturing flaws, environmental damage, or incorrect positioning.
- **Rapid obsolescence:** Older systems soon become obsolete due to rapidly changing technology, which affects long-term investment.

- **Security and privacy risks:** Protective measures and encryption are necessary to prevent unauthorized access to data.
- **Virus attacks:** RFID systems connected to databases are susceptible to hacking attempts and malware.

1.16 Conclusion

In this chapter, we have provided a general scope of the basics of an RFID system, including the tag and the reader by providing their essential characteristics. We have also introduced its various applications, such as healthcare, access control, and automatic toll collection, that make it a valuable identification technology. In addition, we have discussed passive UHF RFID, highlighting its benefits and limitations in different contexts.

Chapter 2

Antenna fundamental parameters of RFID system

Sommaire

2.1 Introduction

This section focuses on an essential component in RFID systems, which is the antenna. Antennas are crucial devices that transmit or receive electromagnetic waves [50]. Positioned at the end of the transmission chain, the antenna is essential to enable communication between the tag and the reader. In this chapter, we will specifically examine antennas used in both readers and tags. This chapter first reviews antenna characteristics, particularly patch antennas. Next, we describe various techniques used to feed patch antennas, which are important in determining their bandwidth and radiation. In addition, we focus on the meandering strategy and, finally, on the impedance-matched antenna.

2.2 Antenna parameters

The antenna serves the purpose of converting the electrical energy of a signal into electromagnetic energy and vice versa. Energy is transferred from the transmitter to free space, where it propagates, with the help of a transmitting antenna. On the other hand, a receiving antenna ensures the transmission of the energy of a wave propagating in space to a receiving device [51]. Therefore, the characteristics of an antenna can be classified into two categories based on the types of energy: electrical characteristics and radiation characteristics.

2.2.1 Electrical parameters

The electrical parameters describe the antenna as a component within its connected circuit. They enable the assessment of the load which the antenna imposes on the circuit and assess how effective power is transferred between the antenna and the radio system. These include metrics like input impedance, the reflection coefficient, the standing wave ratio, the bandwidth, the quality factor, and the noise temperature [51].

2.2.1.1 The input impedance of an antenna

The input impedance Z_{in} is defined as the ratio of the input voltage to the input current at the antenna's terminals:

$$Z_{in} = \frac{V}{I} \tag{2.1}$$

An antenna's input impedance can be broadly represented using the following model in Cartesian form:

$$Z_{in} = R_{in} + jX_{in} = R_R + R_L + jX_{in} \tag{2.2}$$

where,
R_{in}: The resistive part of the antenna
R_R: The radiation resistance (The energy radiated by the antenna)
R_L: The loss resistance (The conduction losses, dielectric losses, and surface wave of the antenna)

X_{in}: Represents the reactive part of the antenna, where:

$$X_{in} = L\omega - \frac{1}{C\omega}$$

ω: Angular frequency ($\omega = 2\pi f$).
The radiation resistance R_R should be zero, and R_{in} should equal the transmission line characteristic impedance [51].

The imaginary part corresponds to the energy stored in the near-field region. If the matching conditions are not met, waves are reflected back toward the source, resulting in standing waves, measured by the Standing Wave Ratio (SWR) (discussed later). The amount of power an antenna radiates depends on the current flowing through it, with the highest radiation occurring at peak current. When the antenna is resonant, its impedance should be minimized to remain purely resistive. For optimal impedance matching ensuring maximum power transfer between the transmission line and the antenna the loss resistance R_P should be zero, and the radiation resistance R_r should equal the transmission line's characteristic impedance [51].

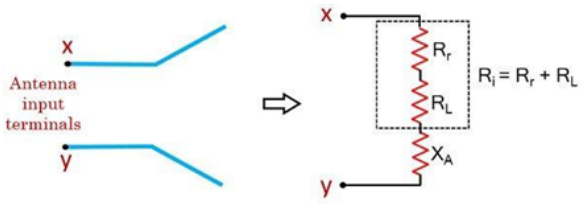

Figure 2.1: Input impedance of antenna.

The efficiency of an antenna can be defined as:

$$\eta = \frac{R_{radiative}}{R_{radiative} + R_{loss}} \tag{2.3}$$

To obtain better efficiency, the resistance linked to losses must be smaller than the resistance linked to radiation.

2.2.1.2 Reflection coefficient and the standing wave ratio

The reflection coefficient shows how much of an electromagnetic wave is reflected by an impedance discontinuity in the transmission medium. The reflection coefficient is equal to the ratio of the amplitude of the reflected wave (the wave returning to the generator) to the incident wave (the wave coming from the generator) [52].

$$\Gamma(x = l) = S_{11} = \frac{Z_{Ant} - Z_c}{Z_{Ant} + Z_c} \tag{2.4}$$

The line is matched if $Z_{Ant} = Z_c$. In this case, 100% of the power is perfectly transmitted to the load and there is no mismatch loss. The significance of impedance matching are shown when: impedances are significantly out of balance, the majority of the power

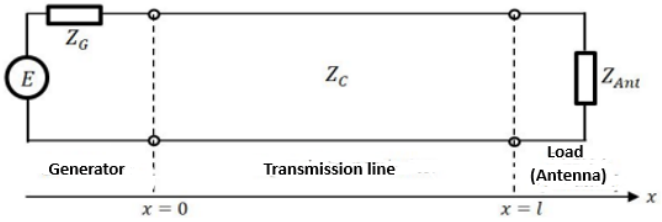

Figure 2.2: The schematic equivalent of an antenna connected to a generator by a transmission line.

will be reflected away from the load (the load is an antenna in our case). The amplitude of the reflection coefficient S_{11} in decibels (dB) is:

$$|S_{11}|_{(dB)} = 20\log|S_{11}| \tag{2.5}$$

VSWR, or standing voltage wave ratio, measures the efficiency of the antenna system in transferring power from the transmitter to the antenna by dividing the greatest voltage point of the antenna by its minimum voltage point. It can be found:

$$\text{VSWR} = \frac{1+|S_{11}|}{1-|S_{11}|} \tag{2.6}$$

An impedance mismatch between the transmitter and the antenna, indicated by a high VSWR, could result in worse transmission and reception quality [52].

2.2.1.3 The bandwidth

The bandwidth or passband of an antenna is the frequency range in which the reflection coefficient remains below a specified threshold. It can also be described as the range of frequencies where the energy transfer between the power source and the antenna (or from the antenna to the receiver) surpasses a defined limit, ensuring proper matching between the excitation source and the antenna.

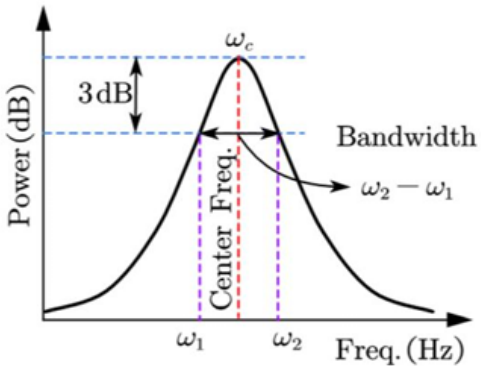

Figure 2.3: The -3dB bandwidth representation [53].

An antenna's bandwidth is typically determined from its reflection coefficient curve or, in some cases, its VSWR curve. It is generally defined by a reflection coefficient below -6 dB, -10 dB, or -15 dB, depending on the chosen criteria. However, the most widely used standard is the -10 dB threshold [54, 55], which means that 90% of the energy from the source is successfully delivered to the antenna, with only 10% being reflected. The bandwidth is commonly viewed as a frequency range centred around the central frequency f_c, the bandwidth Δf is given by [51]:

$$\Delta f = f_2 - f_1 \tag{2.7}$$

Where f_1 and f_2 are the inferior and superior cutoff frequencies, respectively, at a given threshold. The relative fractional bandwidth FBW is a percentage expressing the ratio of the band to the center frequency fc is expressed by:

$$\text{FBW}(\%) = \frac{\Delta f}{f_c} \times 100 \tag{2.8}$$

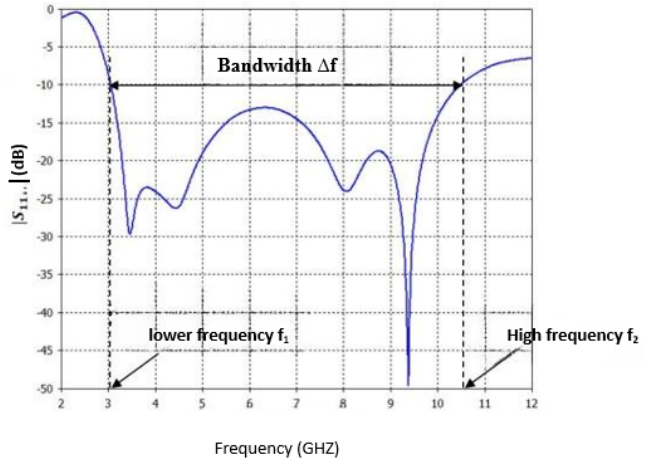

Figure 2.4: Estimation of the bandwidth of an antenna from its reflection coefficient curve.

2.2.1.4 Quality factor

The quality factor is a key property of an antenna, defined by analogy with linear electronic circuits. It is usually calculated at the resonance and connected to the bandwidth. The quality factor represents the losses in the antenna, which include: radiation losses, conduction losses, dielectric losses, and surface wave losses. Thus, the total quality factor is impacted by all these types of losses and it is expressed by [51, 56]:

$$\frac{1}{\text{Q}_t} = \frac{1}{\text{Q}_{rad}} + \frac{1}{\text{Q}_c} + \frac{1}{\text{Q}_d} + \frac{1}{\text{Q}_{sw}} \tag{2.9}$$

where:
Q_t = total quality factor.

Q_{rad} = quality factor due to radiation(space wave) losses.
Q_c = quality factor due to conduction (ohmic) losses.
Q_d = quality factor due to dielectric losses.
Q_{sw} = quality factor due to surface waves.

2.2.2 Radiation parameters

The radiation parameters of an antenna define how it transmits or receives electromagnetic waves in space. The following characteristics are some of the most important radiation characteristics in the antenna:

2.2.2.1 Radiation pattern

The antenna radiation pattern, or in other words, the antenna pattern, is a mathematical function or graphical representation of the radiation properties of the antenna as a function of space coordinates. In the most common case, antenna radiation patterns are determined in the far-field region. This region is where the angular field distribution is essentially independent of the distance from a specified point in the antenna region. The parameter represented by the radiation pattern is typically a normalized magnitude of the pattern function or one of its components, the directivity or partial directivity, or the gain or partial gain – but it may be the phase of a polarization-phase vector component, the axial ratio, or the tilt angle as well; these parameters are reviewed in the following subsections [57].

2.2.2.2 Radiation characteristic function

The radiation characteristic function (RCF), denoted $F(\theta,\phi)$, is a graphical representation of the ratio between the power radiated by the antenna in a specific direction defined by angles θ and ϕ, and the maximum power $P(\theta_0,\phi_0)$ radiated by the same antenna. In other words, RCF is a normalized pattern varies between 0 and 1 in real values (up to 0 in decibels). This depends on the considered direction [51].

$$F(\theta,\phi) = \frac{P(\theta,\phi)}{P(\theta_0,\phi_0)} \tag{2.10}$$

Typically, there are three main forms of radiation patterns which are:

a)isotropic radiation
The definition of an isotropic radiator is "a hypothetical lossless antenna having equal radiation in all directions." It is frequently used as a reference for defining the directional features of real antennas, even though it is ideal and not physically possible Figure 2.6 illustrates it.

b)directional radiation
An antenna with the ability to emit or receive electromagnetic waves more efficiently in certain directions than others is called a directional antenna. This word is typically used to describe an antenna whose maximum directivity is much higher than that of a half-wave dipole. Figure 2.6 illustrates a directional radiation pattern.

c)omnidirectional radiation

An omnidirectional antenna is known for its ability to radiate with equal strength in all directions within a plane. The monopole antenna serves as a classic example of such an antenna. Figure 2.7 illustrates a typical depiction of the omnidirectional radiation pattern.

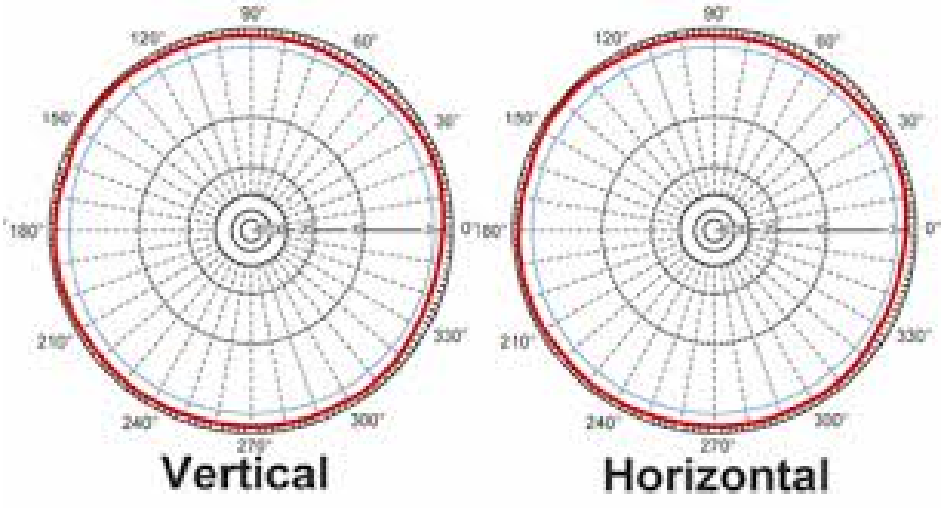

Figure 2.5: Isotropical radiation pattern in vertical and horizontal planes.

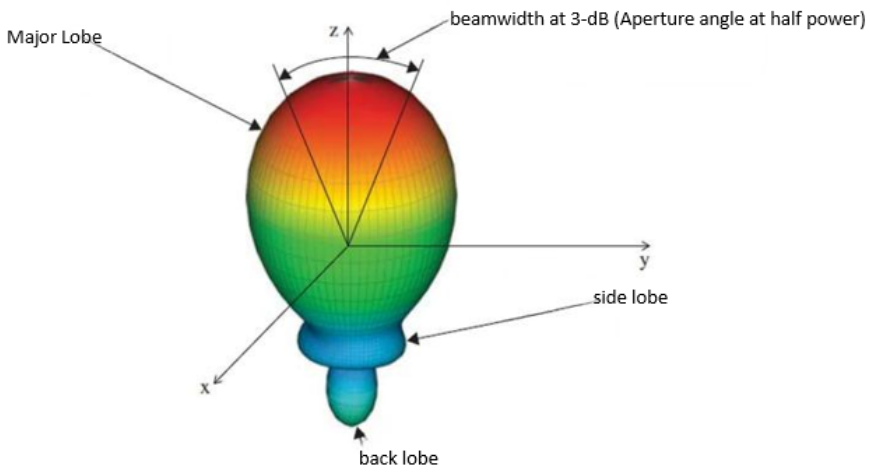

Figure 2.6: Directional radiation pattern in the elevation plane.

2.2.2.3 Half-Power Beamwidth

The half-power beamwidth (HPBW) is identified in a cut of a radiation pattern as the angle between the two directions in which the radiation intensity is half of its maximum value. HPBW characterises the behaviour of the antenna in its main lobe, but it does not take into account the amount of power radiated out of the main beam. For this reason, parameters are normally used to evaluate the antenna's directional performance [57].

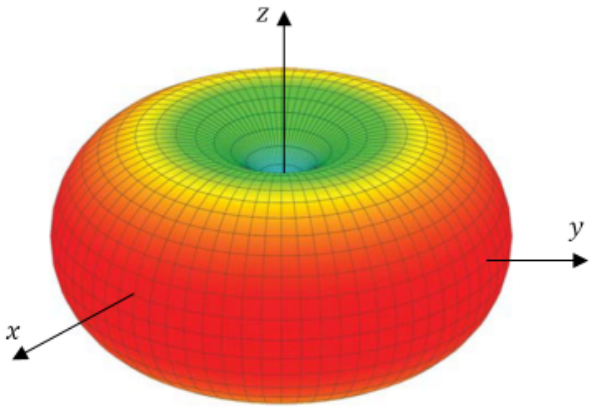

Figure 2.7: Omnidirectional radiation pattern.

2.2.2.4 Field polarization

The polarization of the electromagnetic wave is described by the point locus of the vector electric field E (or magnetic field H) over time, which can distinguish three types of polarization. By taking the z-axis as the propagation direction, the expression on the field is expressed by:

$$\mathrm{E}(z,t) = \hat{x}\mathrm{E}_x(z,t) + \hat{y}\mathrm{E}_y(z,t) \tag{2.11}$$

If the propagation of the wave follows the direction of positive z, the trigonometric form can be written as follows:

$$\mathrm{E}(z,t) = \hat{x}\mathrm{E}_{x_0}\cos(wt - kz + \varphi_x) + \hat{y}\mathrm{E}_{y_0}\cos(wt - kz + \varphi_y) \tag{2.12}$$

Where, E_{x_0} and E_{y_0} are respectively the amplitudes of the electric field E components in the x and y directions; k is the wave number; φ_x and φ_y are the initial phases of the two components E_x, E_y respectively. Three types of polarization are briefly described below [51, 58, 59]:

a)Linear polarization

For the wave to have linear polarization, the time-phase difference between the two components must be

$$\Delta\varphi = \varphi_y - \varphi_x = n\pi, n = 0,1,2,3,... \tag{2.13}$$

Therefore, in trigonometric form it is expressed by:

$$\mathrm{E}(z,t) = \hat{x}\mathrm{E}_{x_0}\cos(wt - kz) \pm \hat{y}\mathrm{E}_{y_0}\cos(wt - kz) \tag{2.14}$$

Figure2.9 represents the orientation of the electric field vector in the linear polarization.

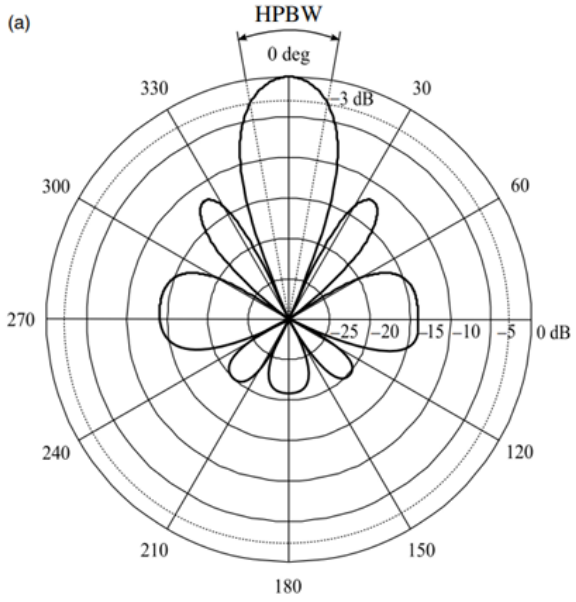

(a) The half-power beamwidth (HPBW).

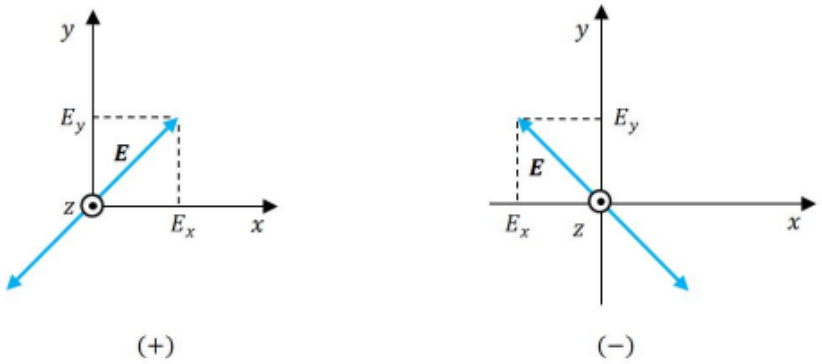

Figure 2.9: Cartesian representation of linear polarization.

b)Circular Polarization

Circular polarization, Figure 2.10, is obtained only when the components of the field vector have the same amplitudes and the phase difference, $\Delta\varphi$, between these two components is an odd number of $\pi/2$.That is,

$$\mathrm{E}_{x_0} = \mathrm{E}_{y0} \tag{2.15}$$

$$\Delta\varphi = \varphi_y - \varphi_x = n\pi = \begin{cases} +(\frac{1}{2}+2n)\pi, n = 1,2,\ldots & \text{for CW} \\ -(\frac{1}{2}+2n)\pi, n = 1,2,\ldots & \text{for CCW} \end{cases} \tag{2.16}$$

c) Elliptical Polarization

In the case of elliptic polarization, if we take only the case of an ellipse aligned on one of the main axes, the amplitudes of the components of the electric field vector are different.Moreover, the phase difference between the two components is an odd multiple of $\pi/2$.That is,

$$\mathrm{E}_{x_0} \neq \mathrm{E}_{y0} \tag{2.17}$$

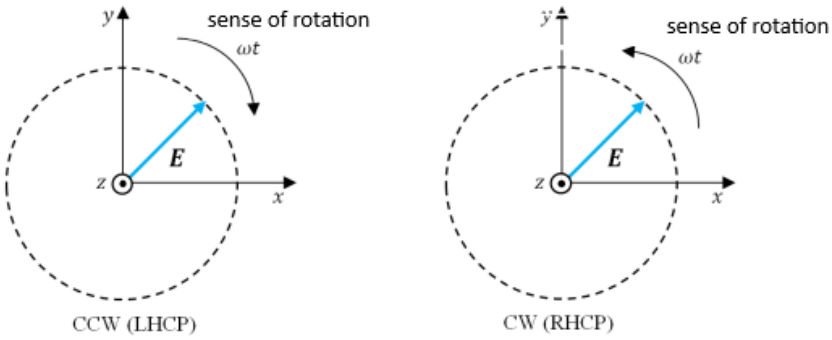

Figure 2.10: Cartesian representation of circular polarization.

and

$$\Delta\varphi = \varphi_y - \varphi_x = n\pi = \begin{cases} +(\frac{1}{2}+2n)\pi, n = 1,2,... & \text{for CW} \\ -(\frac{1}{2}+2n)\pi, n = 1,2,... & \text{for CCW} \end{cases} \tag{2.18}$$

In Figure 2.11, the ellipse is traced by the end of the electric field vector over time.

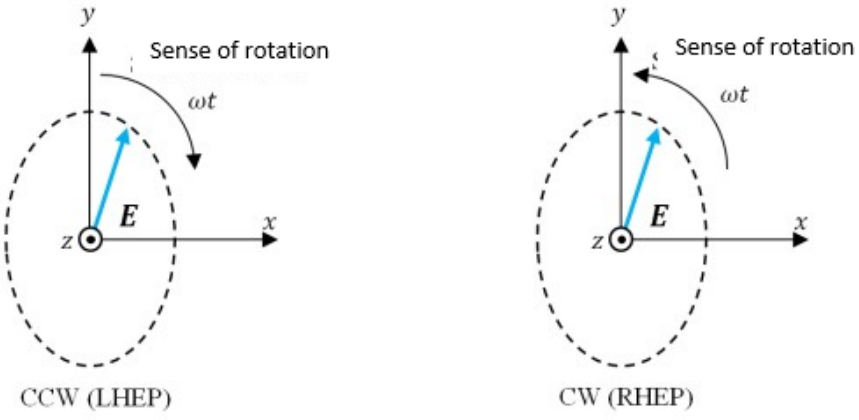

Figure 2.11: Cartesian representation of elliptical polarization.

Knowing that the + and- in the equation respectively represent the left-hand elliptical polarization (RHEP) and the right-hand elliptical polarization (LHEP). In Figure 2.11 the ellipse is plotted by the end of the electric field vector over time. The ratio of the semi-major axis to the semi-minor axis of the ellipse is called the axial ratio. It satisfies the following relationship [51, 58, 59]:

$$\text{AR} = \frac{\text{major axis}}{\text{minor axis}} \tag{2.19}$$

- If AR=1, then the polarization is circular.
- If AR equals to infinite, then the polarization is linear.

AR is often measured in dB:

$$\text{AR}_{dB} = 20\log(\text{AR}) \tag{2.20}$$

If the antenna provides a polarization less than 3dB, it is then considered as circularly polarized.

2.2.2.5 Field regions

The space surrounding an antenna is usually subdivided into three regions: (a) reactive near-field, (b) radiating near-field (Fresnel) and (c) far-field (Fraunhofer) region as shown in Figure 2.12 [60].

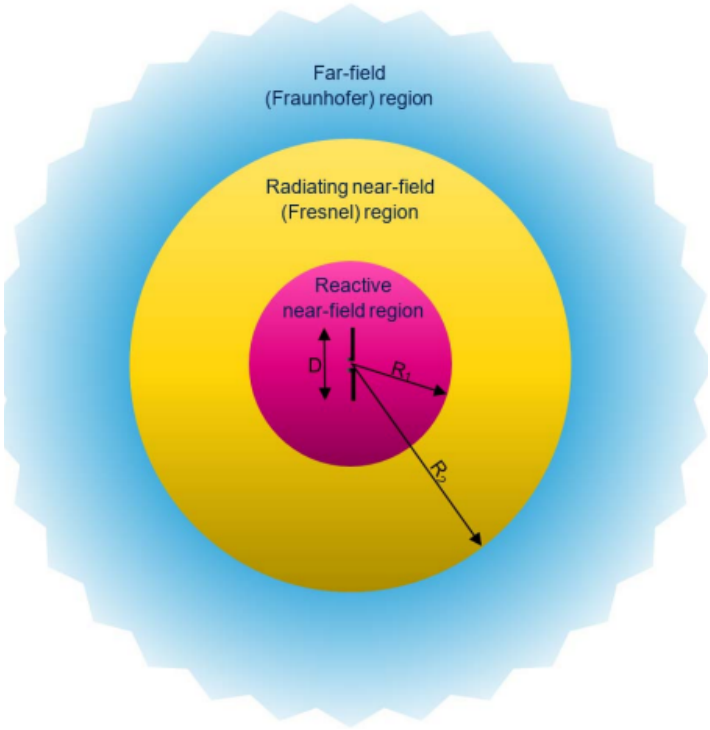

Figure 2.12: Representation of radiation zones.

a)Reactive near-field

The reactive near-field region is the area directly surrounding the antenna where the reactive field dominates. For most antennas, this region can extend up to $R < 0.62\sqrt{D^3/\lambda}$ from the antenna surface, where λ is the wavelength, and D is the antenna's largest dimension. In the case of a very short dipole, this limit is generally considered to be of a very short dipole, or equivalent radiator, which is commonly assumed to exist at a distance of $\lambda/2\pi$ from the antenna surface.

b)Radiating near-field (Fresnel) region

The radiating near-field is located between the reactive near-field region and the far-field region of an antenna. In this zone, radiation fields are dominant, and the angular field distribution depends on the distance from the antenna. Fresnel zone refers to the radiating near-field region of an antenna focused at infinity, based on an optical language analogy. Given that D is the antenna's biggest dimension, the inner boundary is defined as $R < 0.62\sqrt{D^3/\lambda}$ and the outer border as $R < 2D^2/\lambda$. The criterion is predicated on a $\pi/8$ maximum phase inaccuracy. The radial field component may be noticeable in this region, where the field pattern is often a function of the radial distance.

c)far-field region

The far-field region represents the area around an antenna where the angular distribution of the field is unaffected by distance. This region is typically considered to begin at distances greater than $2D^2/\lambda$ from the antenna. However, this distance may not always

be suitable for certain antennas, such as multi-beam reflector antennas, whose far-field patterns are influenced by phase variations across their apertures. In this zone, the field components are primarily transverse, and the angular distribution remains constant regardless of the radial distance at which measurements are taken. The lower boundary of this region is at $R = 2D^2/\lambda$, while the upper boundary theoretically extends to infinity.

2.2.2.6 Antenna Directivity

The directivity of an antenna in a given direction is the ratio between the power radiated in that specific direction and the power that an isotropic antenna would radiate.

The directivity of an antenna is the ratio between the radiation intensity in a given direction and the radiation intensity of an isotropic antenna that radiates the same total power.

$$D(\theta,\phi) = \frac{P(\theta,\phi)}{P_{iso}} = \frac{P(\theta,\phi)}{P_{rad}/4\pi} \tag{2.21}$$

If the direction is not specified, it implies the direction of maximum radiation intensity (maximum directivity) expressed as

$$D_{max} = D_0 = \frac{P_{max}}{P_{iso}} = \frac{4\pi P_{max}}{P_{rad}} \tag{2.22}$$

2.2.2.7 Antenna gain

The gain of an antenna differs from its directivity only by the efficiency η of the antenna:

$$G(\theta,\varphi) = \eta \times D(\theta,\varphi) \tag{2.23}$$

In general, the gain corresponds to the gain in the direction of maximum radiation. This property characterizes the ability of an antenna to focus radiated power in a specific direction. Gain is expressed in decibels (dB) as follows:

$$G_{(dB)} = 10\log_{10}(G) \tag{2.24}$$

The radiation intensity that corresponds to the isotropically radiated power is calculated by dividing the power that the antenna accepts (input) by 4π. Equation form allows for this to be stated as

$$G = 4\pi \frac{\text{radiation intensity}}{\text{total input (accepted) power}} = 4\pi \frac{P(\theta,\phi)}{P_{in}} \tag{2.25}$$

2.2.2.8 Radiation efficiency

The radiation efficiency η, of an antenna measures the part of the power lost between the RF source and the propagation medium. It represents the ratio of the total radiated power P_r to the feed power P_a supplied to it [51].

$$\eta = \frac{P_r}{P_a} \tag{2.26}$$

The gain is then related to the directivity in real values by:

$$G = \frac{P(\theta,\phi)}{P_a/4\pi} = \eta \frac{P(\theta,\phi)}{P_r/4\pi} = \eta D((\theta,\phi) \tag{2.27}$$

2.2.2.9 Friis Transmission Equation

A telecommunication system is made up of a gain antenna G_t, powered by a power P_t and receiving by a gain antenna G_r, located at an emission antenna station. The station has been closed since then is [51]:

$$p_r = \frac{P_t G_t}{4\pi d^2} \tag{2.28}$$

The power received, P_r, by a receiving antenna of surface equivalent to Ar to a distance d is then [51]:

$$P_r = p_r A_r, \text{where } A_r = \frac{G_r \lambda^2}{4\pi} \tag{2.29}$$

The telecommunications equation (Friis' formula) is, therefore:

$$P_r = P_t G_t G_r \left(\frac{\lambda}{4\pi d}\right)^2 \tag{2.30}$$

This yields the Friis formula, which provides the free-space path loss A_0:

$$A_0 = \frac{P_r}{P_t} = \left(\frac{\lambda}{4\pi d}\right)^2 G_t G_r \tag{2.31}$$

The first factor in this expression is called propagation loss.

2.3 Patch antenna

2.3.1 Overall

Nowadays, microstrip patch antennas or patch antennas are widely adopted worldwide [55]. This type of antenna first developed in 1970s. Its flat profile and reduced weight, compared to parabolic reflectors and other antenna options, made it attractive for airborne and spacecraft applications. More recently, the use of materials with high dielectric constant has enabled further miniaturization, making patch antennas a popular choice in mobile devices, GPS receivers and other mass-produced wireless technologies.

2.3.2 Basic patch antenna design

A microstrip patch antenna (MPA) mades up of a conducting patch which can have a planar or nonplanar geometry on one side of a dielectric substrate. This substrate id characterised by a relative dielectric permittivity μ_r and a relative magnetic permeability μr. In the other side of the substrate lies a ground plane includes a metallic engraving that supports surface currents as shown in Figure 2.13, generating electromagnetic radiation. These Currents are transmitted via a microstrip line from the generator to the antenna.

2.3.3 Dielectric materials

Dielectric materials are often used as an intermediate layer between the radiating element and the surface [51]. A dielectrics characterized by two basic parameters; the dielectric constant ϵ_r and the loss tangent $tan\delta$ [61]. These materials have a considerable impact on

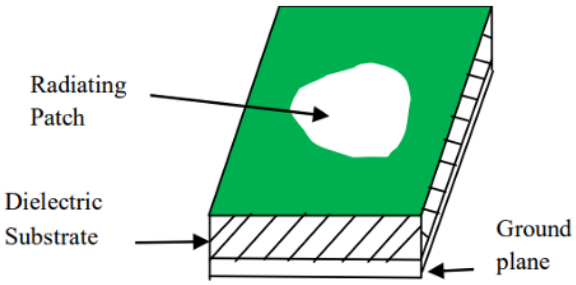

Figure 2.13: Conventional patch antenna geometry [61].

the characteristics of the antenna. The qualities that they need to be used micro-ribbons are [51]:

- Sufficient mechanical strength to support the entire structure.
- Sufficient thermal conductivity to prevent overheating.
- Excellent hydrophobicity, as water impairs material performance.
- Very low dielectric alarms.
- Low dispersion.
- Low anisotropy and linear behaviour.
- One machine and one piece of machinery.

2.3.4 Conductive materials

The section of conductive material is essential as it significantly impact the performance of the patch antenna. Copper is widely used and common due to its high conductivity, resistance to corrosion, and simple method of fabrication. Aluminum is another option, even though its less commonly used compared to copper. Depending on the specific design requirements, other materials with suitable conductivity and fabrication properties may be used. The radiating patch can be designed in several shapes, such as a square, rectangle, thin strip (Dipole), triangle, circular ring, ellipse, or combination of these. Figure 2.14 provides effective examples of these shapes. Although each shape has unique properties, the most used shapes are square, rectangular, and circular due to their ease of production and analysis [62].

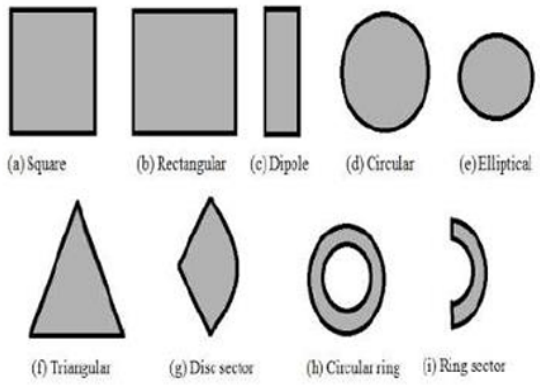

Figure 2.14: Representative shapes of microstrip patch antenna.

2.4 Feeding techniques for patch antennas

A feedline is used to excite to radiate by direct or indirect contact. There are many different techniques of feeding, and the four most popular techniques are coaxial probe feed, microstrip line, aperture coupling and proximity coupling [61].

2.4.1 Coaxial probe feeding

Coaxial probe feeding is a feeding method in which the inner conductor of the coaxial is attached to the radiation patch of the antenna while the outer conductor is connected to the ground plane. Advantages of coaxial feeding is easy of fabrication, easy to match, low spurious radiation and its disadvantages is narrow bandwidth, Difficult to model specially for thick substrate Figure 2.15 [61].

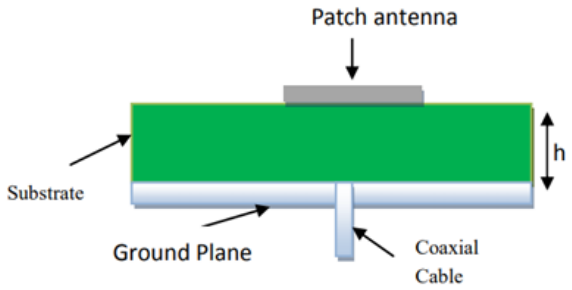

Figure 2.15: coaxial probe feeding [61].

2.4.2 Microstrip line feed

Microstrip line feed is one of the easier methods to fabricate as it is just a conducting strip connecting to the patch and, therefore, it can be considered as an extension of the patch. It is simple to model and easy to match by controlling the inset position. However, the disadvantage of this method is that as substrate thickness increases, surface wave and spurious feed radiation increases, which limits the bandwidth [61].

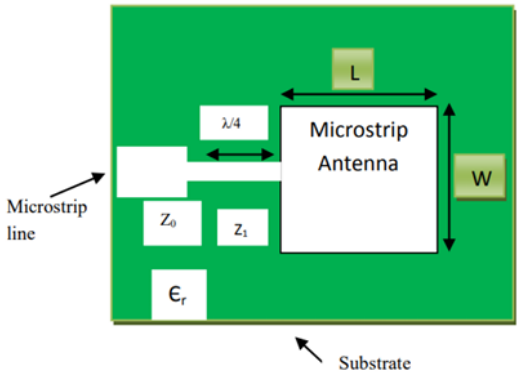

Figure 2.16: Microstrip line feed patch antenna [61].

2.4.2.1 Aperture coupled feed

Aperture-coupled feed consists of two different substrates separated by a ground plane. On the bottom side of the lower substrate, there is a microstrip feed line whose energy is coupled to the patch through a slot on the ground plane separating the two substrates. This arrangement allows independent optimisation of the feed mechanism and the radiating element. Normally, the top substrate uses a thick low dielectric constant substrate, while the bottom substrate is the high dielectric substrate. The ground plane, which is in the middle, isolates the feed from the radiation element and minimizes the interference of spurious radiation for pattern formation and polarization purity. The advantage is that it allows independent optimisation of the feed mechanism element [61].

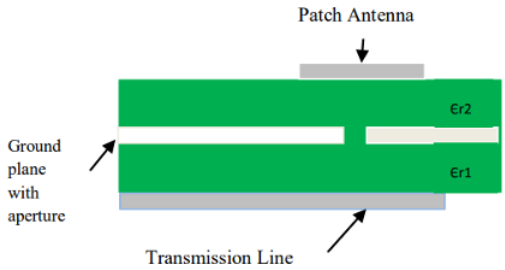

Figure 2.17: Aperture coupled feed patch antenna [61].

2.4.2.2 Proximity coupling

Proximity coupling has the largest bandwidth and low spurious radiation. However, its fabrication is difficult. The length of the feeding stub and the width-to-length ratio of the patch is used to control the match. Its coupling mechanism is capacitive in nature [61].

The major disadvantage of this feeding technique is that it is difficult to fabricate because of the two dielectric layers that need proper alignment. Also, there is an increase in the overall thickness of the antenna. In the wide range of antenna models, there are different structures of Microstrip antennas, but on the whole, we have four basic parts in the antenna [61]:

They are:

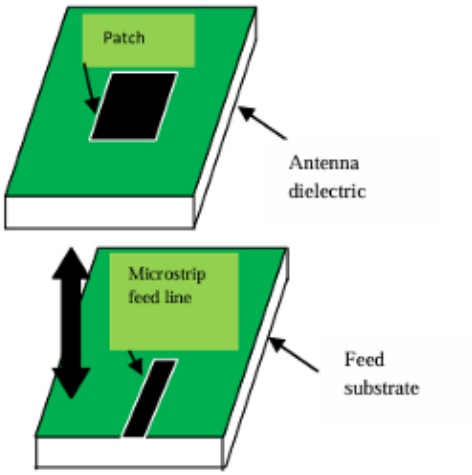

Figure 2.18: Proximity coupled microstrip patch antenna [61].

- The patch
- Dielectric Substrate
- Ground Plane
- Feed Line

The characteristics of microstrip patch antennas, microstrip sot antennas and printed dipole antennas are summarized compared in table 2.1 [61]:

Table 2.1: Characteristics comparison

Characteristics	Microstrip patch antenna	Microstrip slot antenna	Printed dipole antenna
Profile	thin	thin	Thin
Fabrication	Very easy	easy	easy
Polarization	Both linear and circular	Both linear and circular	linear
Dual-frequency operation	possible	possible	possible
Shape flexibility	Any shape	Mostly rectangular and circular shapes	Rectangular and triangular
Spurious radiation	Exists	Exists	Exists
Bandwidth	2–50%	5–30%	~30%

2.5 Types of patch antenna arrays

Sometimes, the use of a single patch is insufficient to meet the constraints of radiation. To improve antenna performance, a multilayer structure that allows an increase in the

bandwidth and combines the different radiant elements forms a system called a network. This makes it possible to compensate for the limitations of the characteristics of a single antenna by playing on many factors, such as the spacing and phase of the patches and the size of the ground plane, to have a higher gain and a conforming main lobe. Figure 2.19 identifies three typical configurations of antenna arrays, which are linear, planar and circular arrays [51, 63, 64].

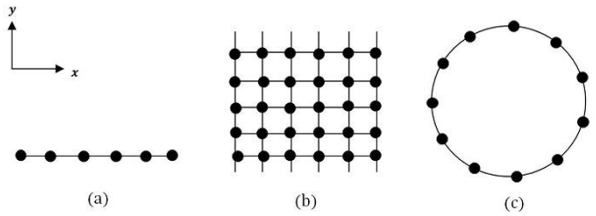

Figure 2.19: Different geometric configurations of antenna arrays: (a) linear, (b) planar and (c) circular [51].

2.5.0.1 Linear array

In a linear array, the radiating elements are placed one after the other through a parallel displacement along the same line, as shown in Figure 2.19.a

2.5.0.2 Planner array

In a planar network, the radiating elements are deduced from each other through parallel translations on the same plane as shown in Figure 2.19.b.

2.5.0.3 Circular Array Antenna

An antenna consists of a group of identical radiating elements in which each set of points is placed on a circle, Figure 2.19.c explain it.

The parameters considered to control the shape of the overall radiation pattern are:

- The array's geometry (linear, planar, or circular).
- The relative spacing between each element.
- The amplitude of the excitation of each element.
- The phase applied to each excitation.
- The radiation pattern of each element.

2.6 Methods for size reduction

Since most UHF RFID tags must be attached to small objects, the antenna's geometry should be miniaturised without unacceptable degradation of the radiation efficiency. In order to achieve that, meandering strategy and inverted-F structures are proposed. Both

strategies require a single or multiple folding of the radiating body, However, the inverted-F antennas additionally include a finite approximation of a ground plane [65].

2.6.1 The meandering strategy

A wire configuration is produced by folding in the arms of a dipole antenna along a meandered path with distributed capacitive and inductive reactances that globally affect the antenna's input impedance. Up to the first antenna resonance, the currents on the adjacent horizontal segments of mender-line antennas (MLA) have opposite phases. These transmission-line currents do not contribute to the radiated power but produce losses. Resonances are achieved at much lower frequencies than in the case of a straight dipole of the same height, at the expense of a narrow bandwidth and low efficiency [65].

Figures 2.21 shows some relevant examples of RFID tag antennas found in recent scientific publications, which use the meander-line technique to reduce the size.

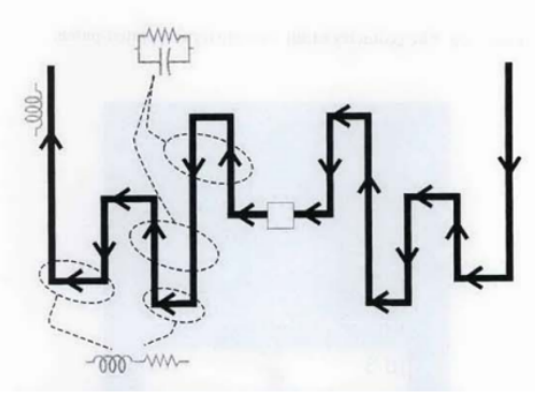

Figure 2.20: The geometry of a meander-line antenna having multiple unequal turns [65].

A meander-line antenna can have periodic shapes or be individually optimized to match a specific impedance, which helps to enhance the performance for a diverse range of applications like RFID and wireless devices.

2.6.2 The F-inverted configuration

The size of a vertical wire monopole can be reduced by folding part of the wire parallel to the ground plane according to an inverted-L structure. Which typically has a low resistance and a high capacitive reactance. To provide tuning freedom, the structure is augmented with a shorting pin, giving the F-type (Inverted F Antenna, IFA) configuration. This can also be viewed as a monopole version of the T-match, where the radiating body is folded to reduce the space occupied.

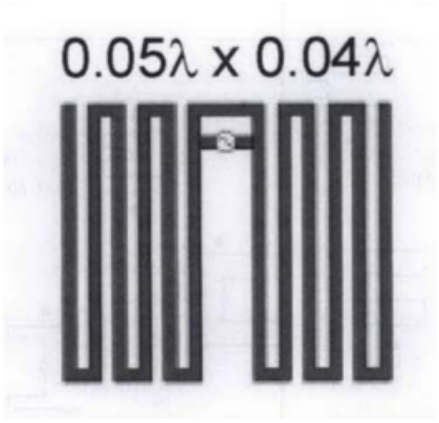

(a) Equi-spaced meander line antenna. Dimensions: 0,05 λ × 0,04 λ and 0,24 λ × 0,05 λ

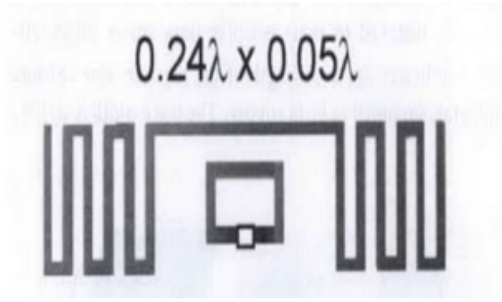

(b) Meander line antenna with coupled loop feed

. Dimensions: 0,24 λ × 0,05 λ

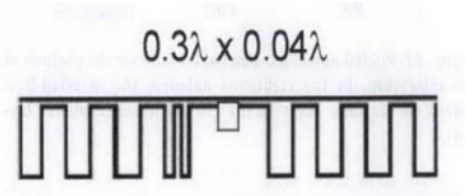

(c) Equi-spaced meander-line with loading bar

. Dimensions: 0,3 λ × 0,04 λ, 0,27 λ × 0,01 λ

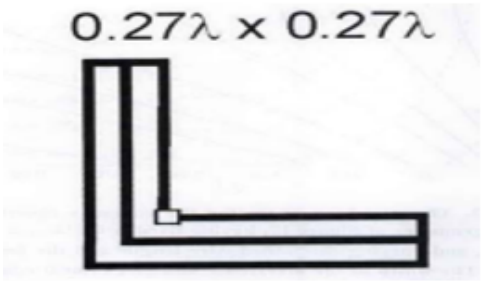

(d) Doubly-folded L-shaped dipole

. Dimensions: 0,22 λ × 0,12 λ

(e) Multiconductor antenna with double T-match

. Dimensions: 0,22 λ × 0,12 λ

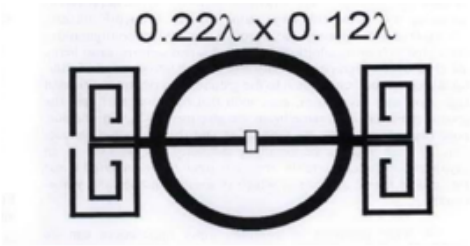

(f) Multiconductor meander-line tag **[22]**. Dimensions: 0,22 λ × 0,12 λ

Figure 2.21: Comparative layouts of meander-line RFID tag antennas with their respective dimensions (wavelength λ scales). Figures (a)-(b) show basic designs, (c)-(d) intermediate configurations, and (e)-(f) advanced matching techniques.

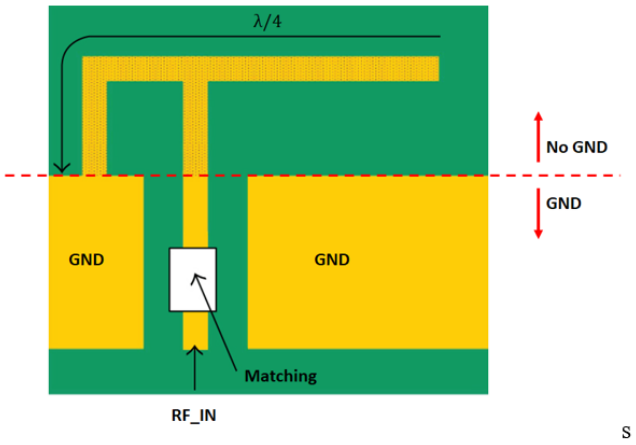

Figure 2.22: Inverted-F antenna.

2.7 Impedance matching

The three types of lumped element matching networks that are commonly used are based on the L-network, π-network, and T-network. The advantage of L-network is that it only has two reactive components whose values can be tuned easily for a given load impedance. However, its impedance matching capability is limited. On the other hand, theπ- or T-networks have the capability of providing superior impedance matching flexibility than the L-network because they have three reactive components that can be tuned.

Figure 2.23 shows equivalent circuit of a typical L- and T-matching networks. The reactive components can be either lumped elements or realized using transmission lines based on microstrip integrated circuit technology. Capacitors can be realized using interdigital or low impedance microstrip lines and inductors can be realized using high impedance microstrip lines. Reactive components realized using microstrip lines can, however, result in a larger circuit size [66].

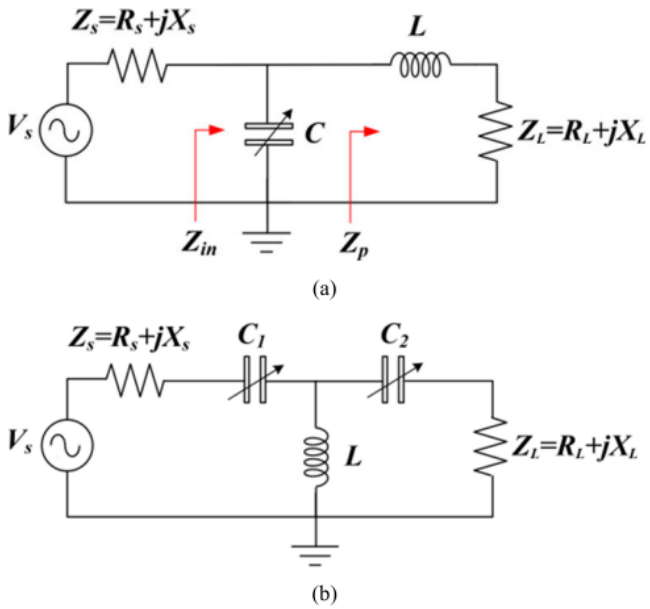

Figure 2.23: (a) Equivalent circuit of L-matching network, and (b) equivalent circuit of T-matching network.

2.8 Conclusion

A theoretical demonstration on antenna parameters and characteristics has been discussed in this chapter, by exposing microstrip patch antenna features and their applications in the RFID systems. Some factors are involved in the selection of feeding techniques. Particular microstrip patch antenna can be designed for each application and different merits are compared with conventional microwave antennas.

Chapter 3

Design of a circularly polarized RFID reader antenna for UHF/SHF applications

Sommaire

3.1 Introduction

In this chapter, we present the design and the simulation of a dual-band circularly polarized (CP) RFID reader antenna. This antenna operates at 0.915 GHz and 2.45 GHz. All the results are obtained by using CST Studio Microwave Software. We start with a parametric study, showing the mean parameters that affect the antenna performance. Then, we show the final results of the optimized reader antenna which demonstrate a high performane for UHS/SHF applications.

3.2 CST Studio Microwave Software

CST is a 3D simulation software used for designing and analyzing electromagnetic systems, It is widely used in fields like antennas, high-frequency circuits, microwaves, and radiation control. It supports both time and frequency domain analysis, showing results like S-parameters and field distributions. Users can create precise 3D models of components such as antennas and filters. It is used in industry and academia to reduce prototyping costs and shorten development time. It is known for its high accuracy and user-friendly graphical interface for design and simulation.

3.3 Design process of the proposed reader antenna

In order to create a circularly polarized RFID reader antenna to cover the UHF/SHF band, we have followed several steps and considerations. Figure 3.1 provides an overview of the design process.

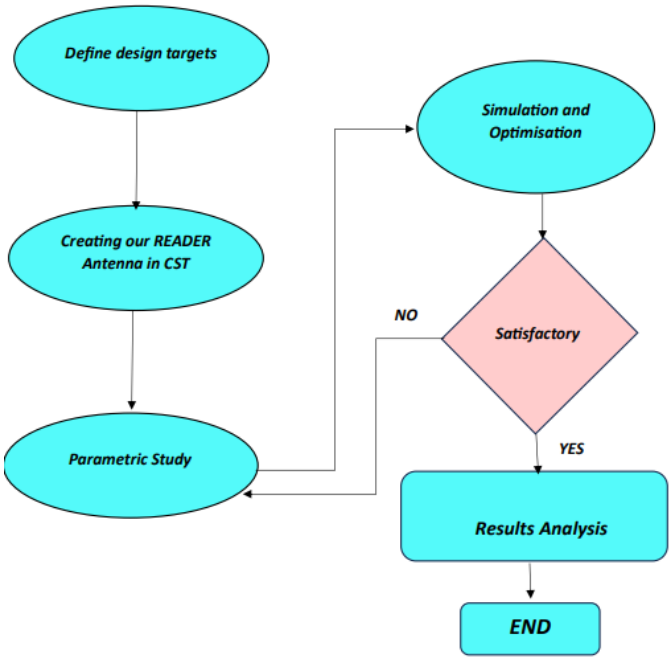

Figure 3.1: The Methodology Flowchart.

3.4 Antenna design

3.4.1 Finalized reader antenna design

The design of the proposed reader antenna is inspired from the sequential phase configuration [10]. The design is implemented on a Rogers 4003c substrate, featuring a relative permittivity of $\varepsilon_r = 3.55$ and a loss tangent of $tan\delta = 0.0027$, with dimensions of $104 \times 104 \times 1.524\ mm^3$. First, we had two L longer-shaped arms. Then, we changed the L-shape by dividing it into five segments and intentionally created an open quasi-rectangular shape at the end of the arm in order to obtain a circular polarization. Additionally, we modified the width and the length of the shorter L-arm to achieve the desired PC and to target the SHF band. Double-sided dipoles are patterned on both the upper and lower surfaces of the substrate, comprising two dipole pairs fed centrally through a 50 Ω coaxial cable. For the upper three-quarter ring delay line, the bottom layer's pink metal serves as the ground plane, whereas for the lower ring, the top red metal layer performs this function. To eliminate blockage caused by the longer dipole over the shorter one figure 3.2. The longer dipole is rotated by 90 degrees. Furthermore, 90° bend is introduced at the end of the longer dipole to reduce the antenna overall footprint. Both dipole pairs are linked via a concentric ring delay line, defined by inner and outer radii denoted r_1 and r_2.

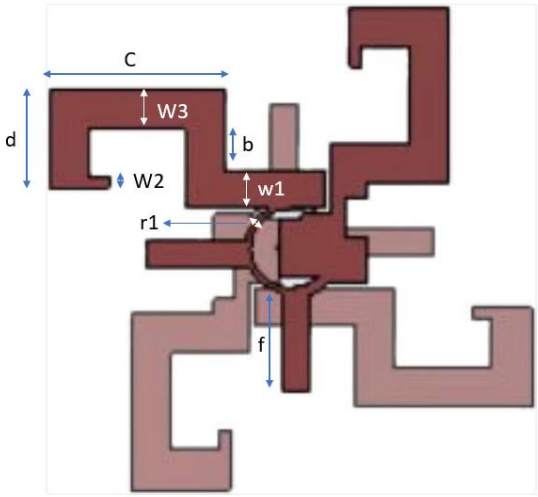

Figure 3.2: Geometry of the proposed reader antenna.

Table 3.1: Dimensions of the proposed reader antenna.

Parameter	s	l_s	c	b	W_1	W_2	W_3	f	a	r_1	d
Value (mm)	104	104	17	14	6.5	2	7.1	2	17.5	7	17.5

3.4.2 Parametric study

3.4.2.1 Axial ratio

Figure 3.3 illustrates the axial ratio (AR) in dB as a function of frequency in GHz for different values of the design parameter denoted W3. The following results show that the configuration with W3= 11 mm achieves the lowest axial ratio at 915 MHz and 2.4 GHz (AR<3 dB), indicating the presence of circular polarization.

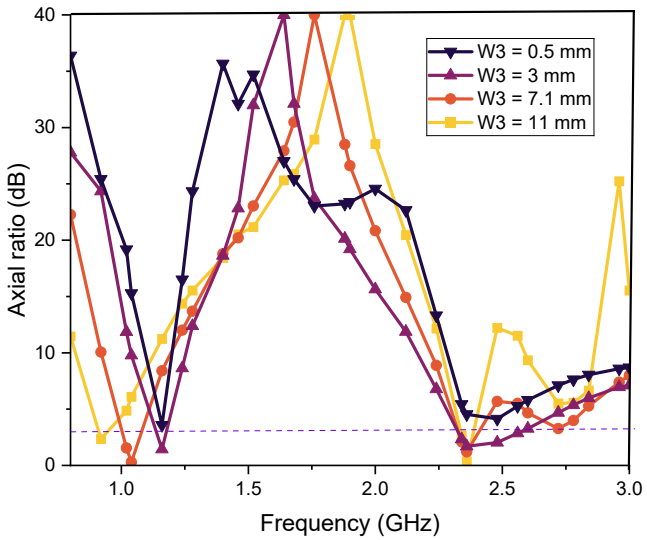

Figure 3.3: Axial ratio (dB) as a function of frequency of the proposed reader antenna.

3.4.2.2 Reflection coefficient

Figure 3.4 represents the line graphs for the first attempts used to obtain effective results of the magnitude of reflection coefficient $|S_{11}|$ as a function of frequency GHz of the proposed RFID reader antenna. The parameter W2 is crucial for enhancing $|S_{11}|$.

3.4.3 Finalized reader antenna

3.4.3.1 Reflection coefficient

Figure 3.5 shows the reflection coefficient for the proposed reader antenna which covers UHF and SHF bands. The value of the return loss for UHF band at 0.915 GHz is -30.87 and for SHF(large band) at 2.4 GHz, 2.8 GHz and 3.7 GHz is -45 dB, -49.39 dB and -27.38 dB, respectively.

3.4.3.2 Axial ratio

Figure 3.6 shows the axial ratio of the proposed reader antenna. The axial ratio within the UHF band is around 1 dB, and for the SHF band is 3 dB. These values demonstrate that the reader antenna performance is good regarding circular polarization.

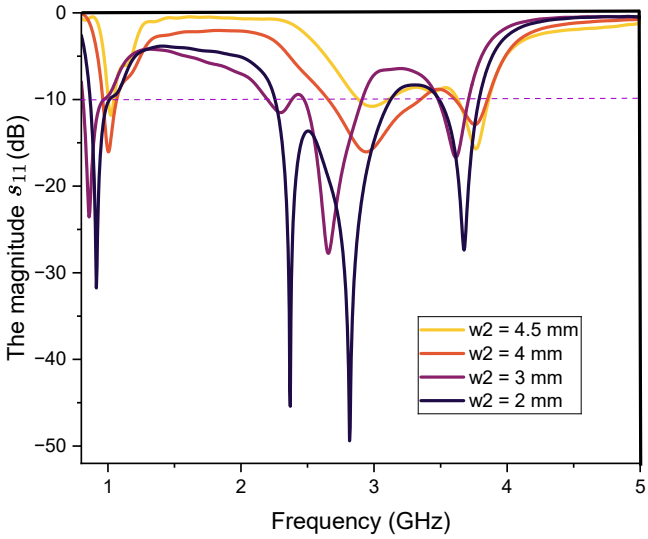

Figure 3.4: The return loss (dB) as a function of frequency of the proposed reader antenna.

3.4.3.3 Electric field

Figures 3.7, 3.8 and 3.9 show the radiated electric field at various instances: $\omega t = 0°$ (figs. 3.7a, 3.8a and 3.9a), $\omega t = 90°$ (figs. 3.7b, 3.8b and 3.9b), $\omega t = 180°$ (figs. 3.7c, 3.8c and 3.9c) and $\omega t = 270°$ (figs. 3.7d, 3.8d and 3.9d). The electric field rotates in RHCP toward $z > 0$, whereas the LHCP of electric field is in $z < 0$. Figures 3.10, 3.11, 3.12 and 3.13 represent the surface current on the reader antenna at 915 MHz, 2.4 GHz, 2.8 GHz and 3.7 GHz, respectively, where the substrate current goes to zero.

3.4.3.4 Realized gain

Figure 3.14 shows the realized gain in dBi versus frequency in GHz for reader antenna. The realized gain in UHF band is 1.73 dBi, for SHF (large band) at 2.4 GHz , 2.8 GHz and 3.7 GHz is 3.41 dBi, 5.9 dBi and 5.72 dBi respectively. These values demonstrate that the reader antenna performance is good in terms of realized gain.

3.4.3.5 Total efficiency

Figure 3.15 shows a graph of the efficiency of reader antenna over a specific bandwidth. The reader antenna shows high efficiency. This latter reaches 98% at 0.915 GHz, which means that 98% of the antenna input is converted into electromagnetic radiation. Also, an efficiency of 96% at 2.4 GHz, 98% at 2.8 GHz and 97% at 3.7 GHz are achieved. This indicates that the antenna radiates efficiently at all frequencies.

3.4.3.6 Radiation Pattern

Our proposed antenna shows directional radiation at 0.915 GHz and 2.4 GHz, as it is shown in the Figure 3.16.

Figure 3.17 shows the radiation pattern in polar representation of the proposed antenna with a maximum gain of 1.73 dBi and 5.9 dBi at 0.915 GHz and 2.4 GHz respectively.

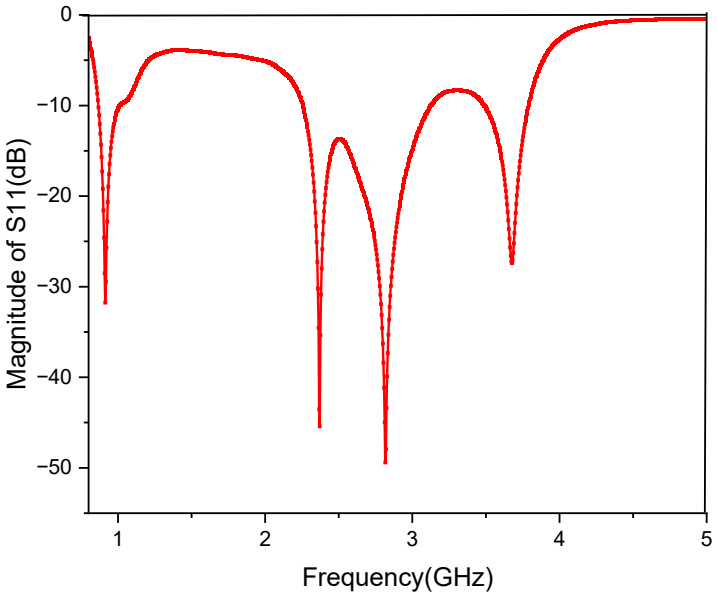

Figure 3.5: The value of $|S_{11}|$ in dB versus frequency in GHz of the proposed reader antenna.

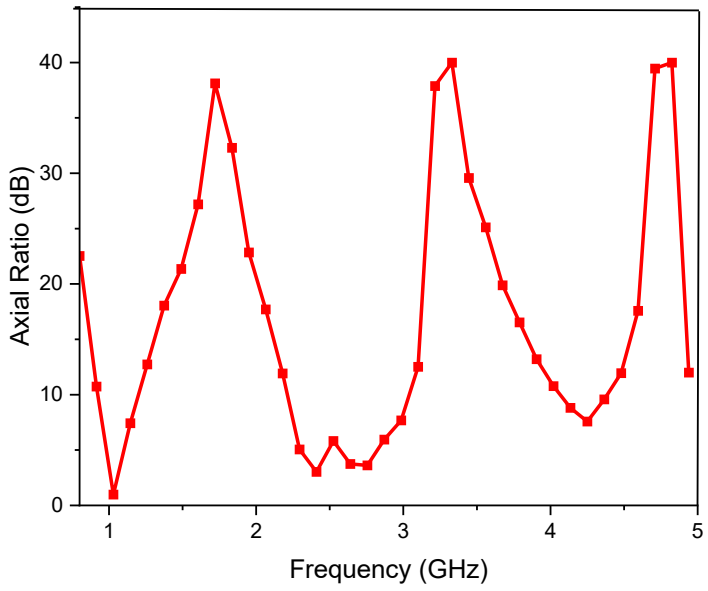

Figure 3.6: The value of axial ratio in dB versus frequency in GHz of antenna.

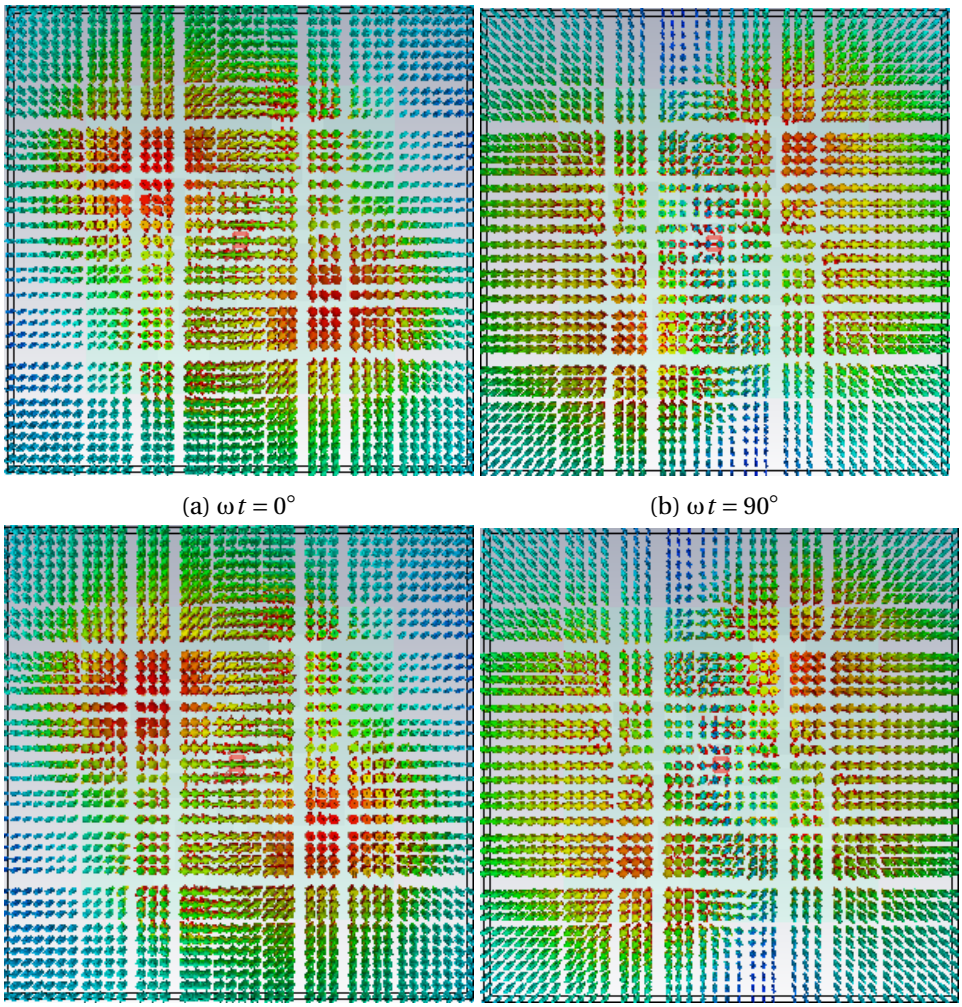

(a) $\omega t = 0°$ (b) $\omega t = 90°$

(c) $\omega t = 180°$ (d) $\omega t = 270°$

Figure 3.7: Radiated electric field at various instances of antenna at 0.915 GHz.

This figure shows a maximum bidirectional radiation at frequency 0.915 GHz and 2.45 GHz at the x-z and y-z planes for $\varphi = 0°$ and $\varphi = 90°$.

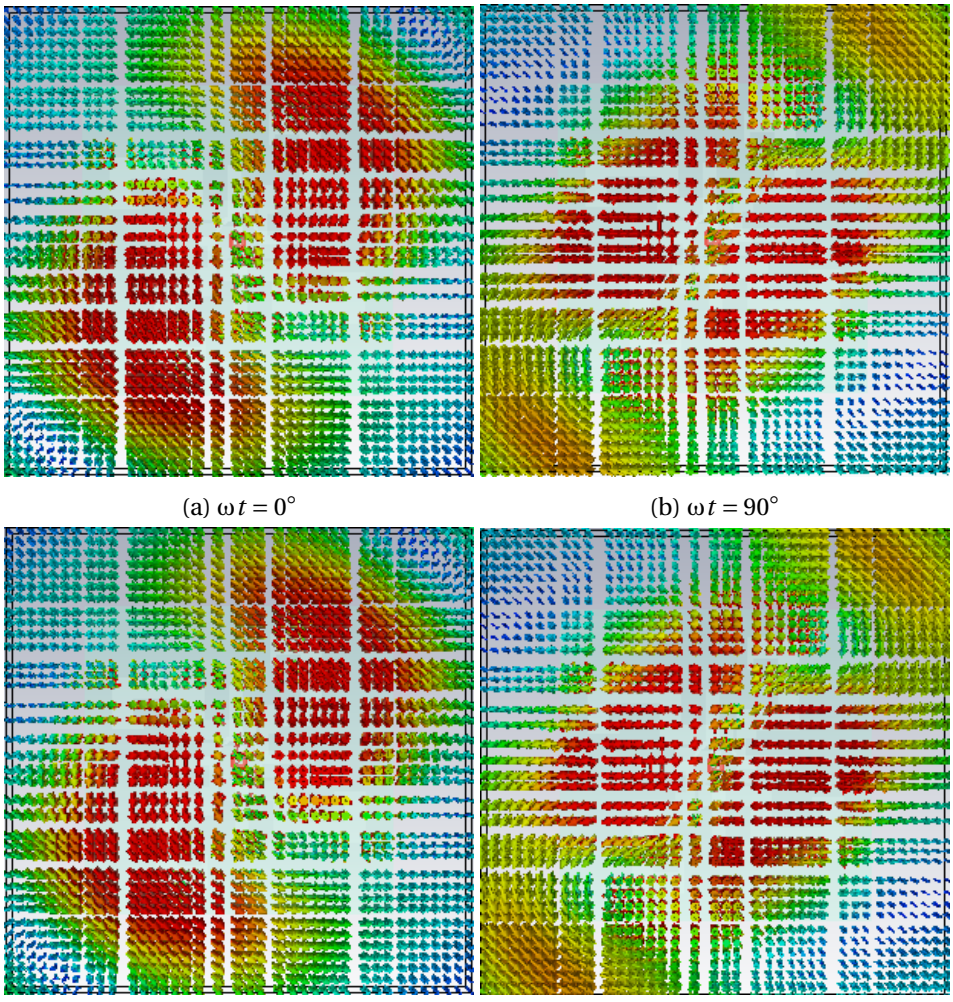

(a) $\omega t = 0°$ (b) $\omega t = 90°$

(c) $\omega t = 180°$ (d) $\omega t = 270°$

Figure 3.8: Radiated electric field at various instances of the proposed reader antenna at 2.4 GHz.

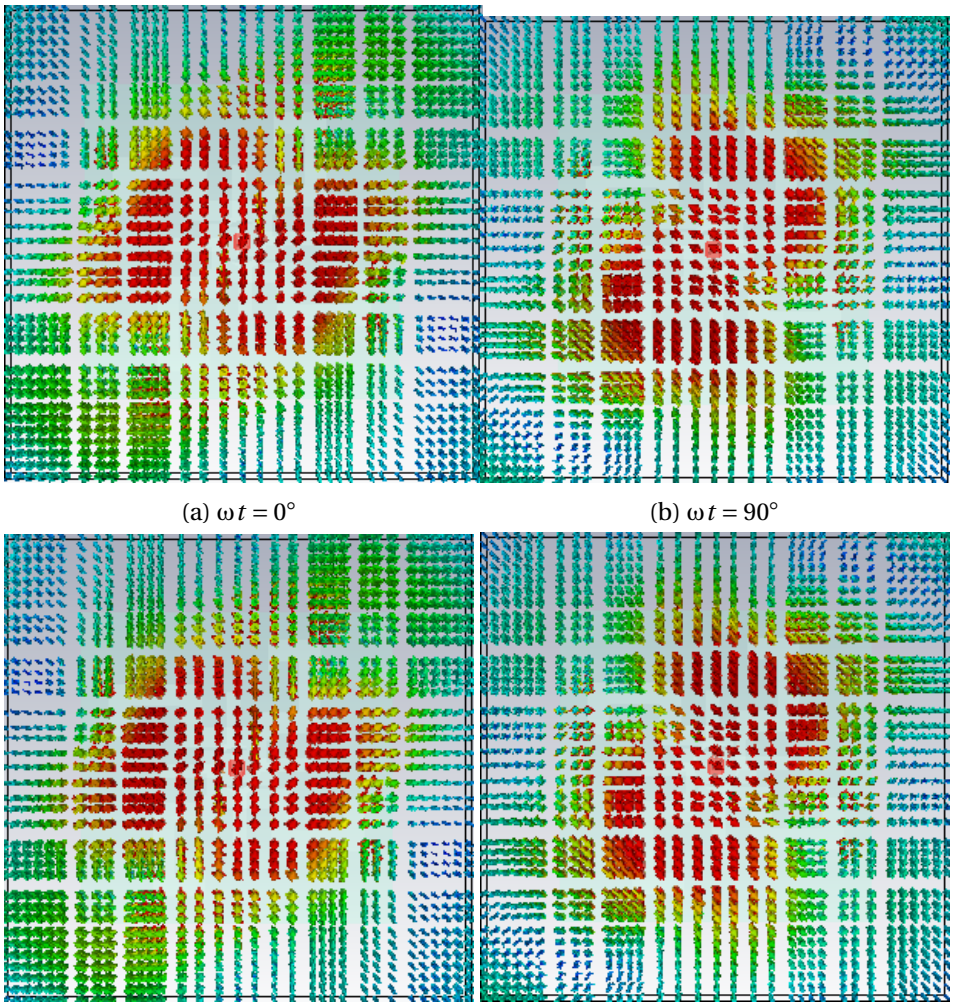

(a) $\omega t = 0°$ (b) $\omega t = 90°$

(c) $\omega t = 180°$ (d) $\omega t = 270°$

Figure 3.9: Radiated electric field at various instances of antenna at 2.8 GHz.

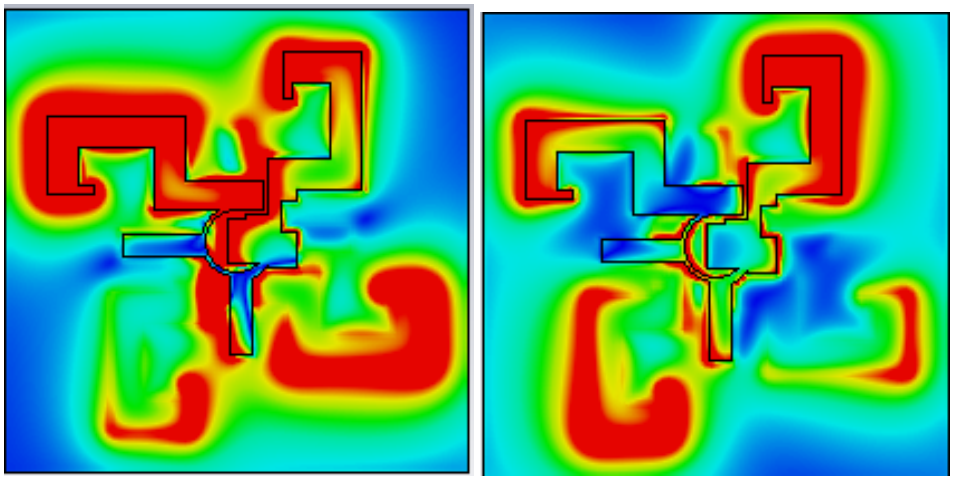

(a) at 0°. (b) at 90°.

Figure 3.10: Surface current of the reader antenna at 0.915 GHz.

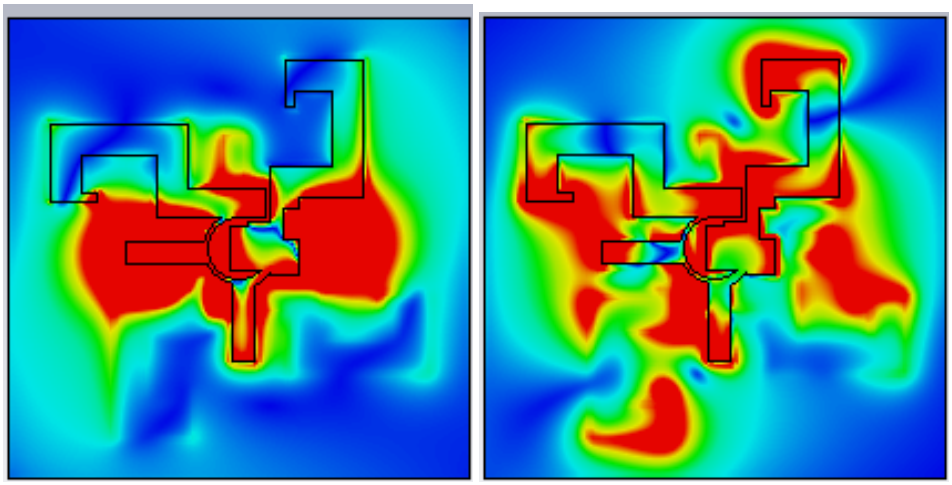

(a) at 0°. (b) at 90°.

Figure 3.11: Surface current of the reader antenna at 2.4 GHz.

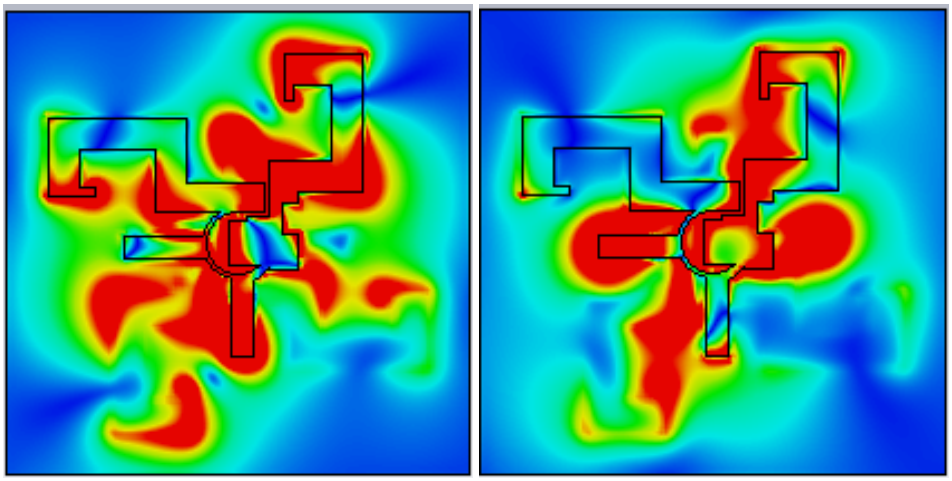

(a) at 0°. (b) at 90°.

Figure 3.12: Surface current of the reader antenna at 2.8 GHz.

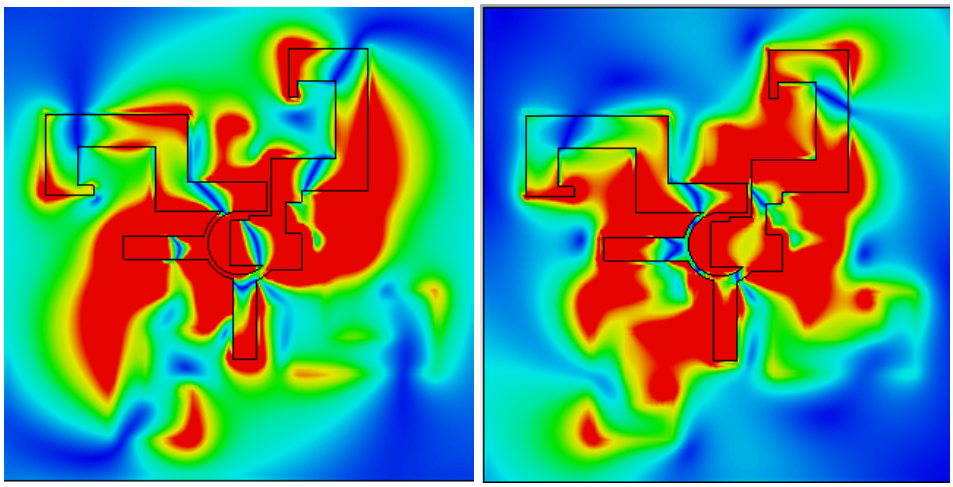

(a) at 0° (b) at 90°

Figure 3.13: Surface current of the reader antenna at 3.7 GHz.

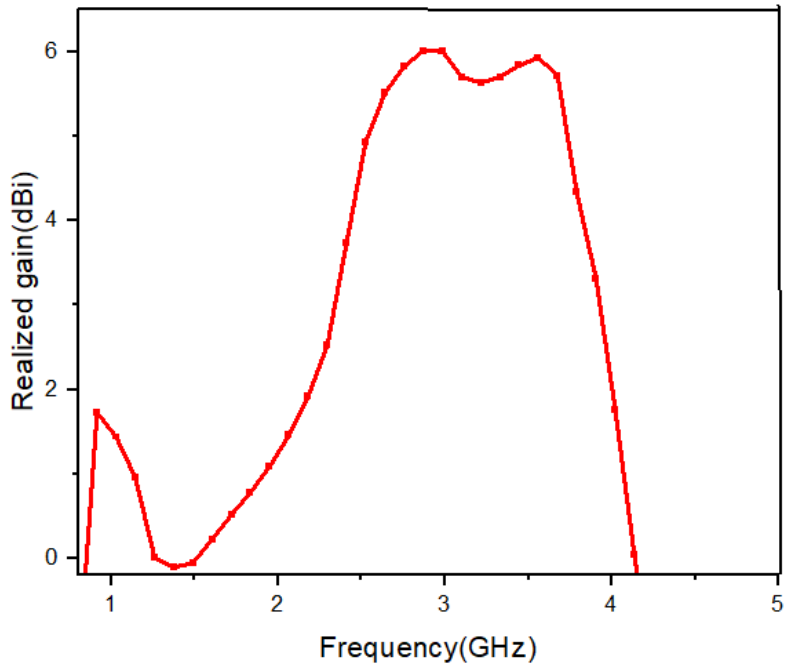

Figure 3.14: The value of realized gain in dBi versus frequency in GHz of antenna.

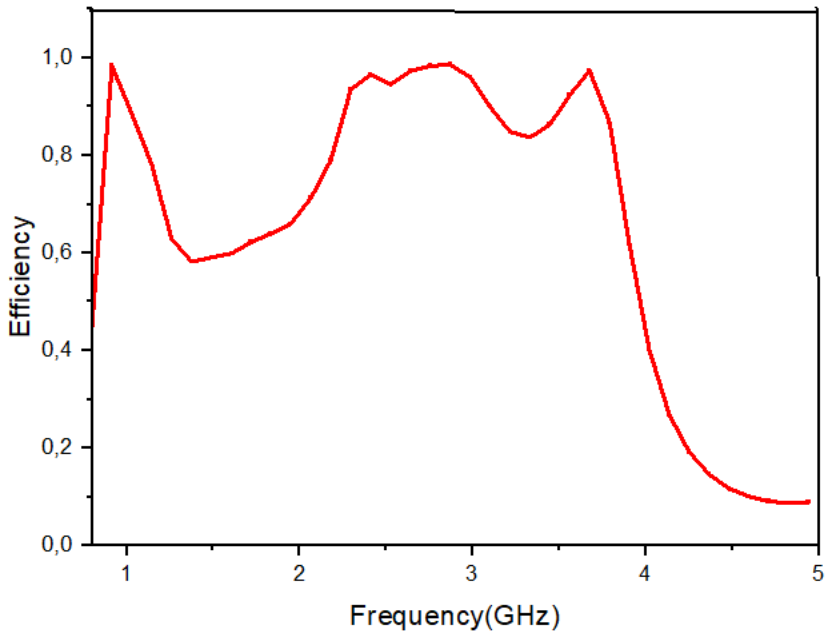

Figure 3.15: The value of efficiency versus frequency in GHz of antenna.

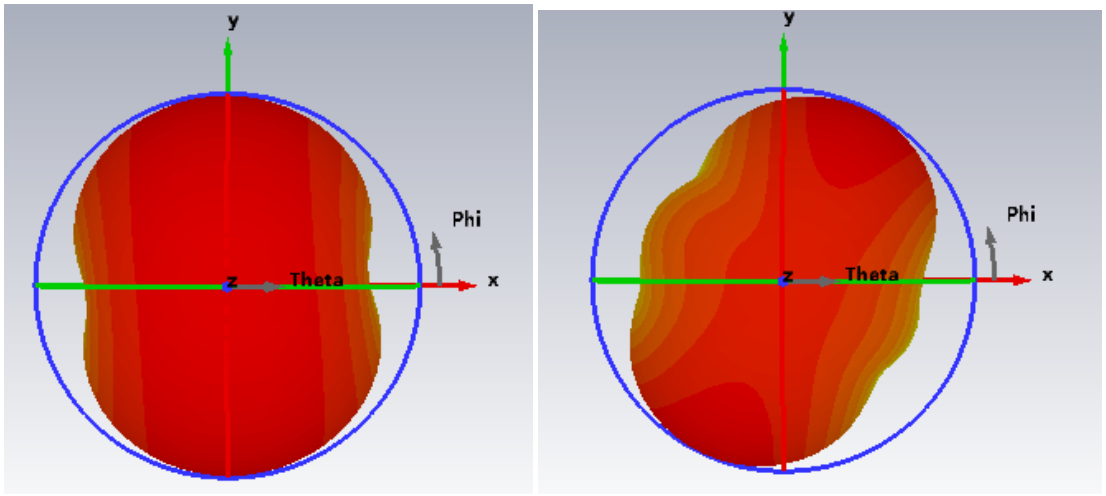

(a) (b)

Figure 3.16: 3D radiation pattern, (a) at 0.915 GHz; (b) at 2.4 GHz.

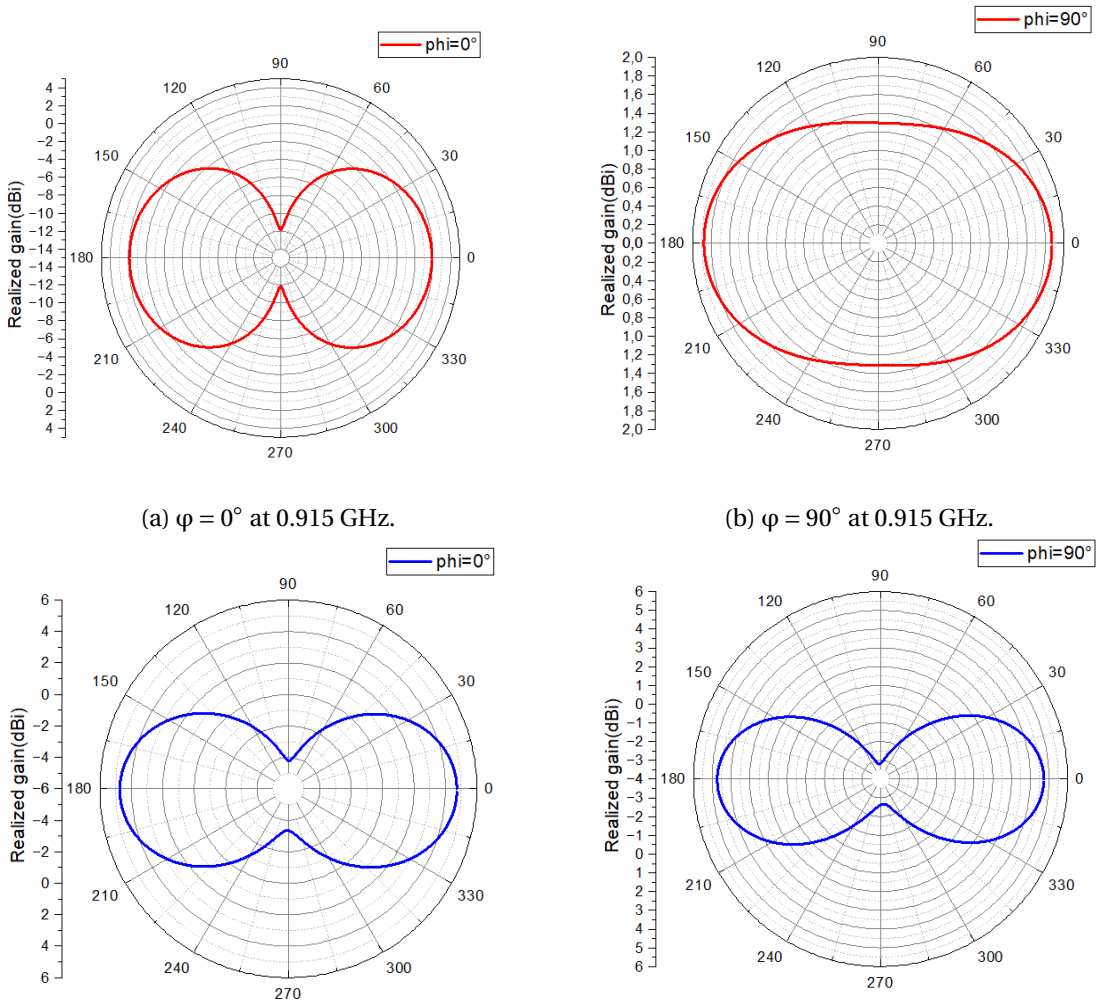

(a) $\varphi = 0°$ at 0.915 GHz. (b) $\varphi = 90°$ at 0.915 GHz.

(c) $\varphi = 0°$ at 2.4 GHz. (d) $\varphi = 90°$ at 2.4 GHz.

Figure 3.17: Radiation patterns of antenna 2 at 0.915 GHz and 2.4 GHz.

3.5 Performance comparison with reported antennas

Table 3.2 represents a comparison between the proposed antenna and those mentioned in literature [8–11], in terms of size, bandwidth, field polarization, and gain. This comparison shows that the proposed antenna has the higher gain of 1.73 dBi at 0.915 GHz and 5.7 dBi at 2.4 GHz and 5.9 at 3.7 GHz compared to the other antennas [8–11]. It has a size of $104 \times 104 \times 1.527\ mm^3$ with a circular polarization for both UHF and SHF bands. As well as, a elliptical polarization at 3.7 GHz is achieved. This performance makes the proposed antenna an excellent candidate for RFID applications operating within UHF/SHF band in CP-radiation.

Table 3.2: Comparison of antenna performance characteristics.

Ref., year	Size (mm^3)	Bandwidth (GHz)	Field Polarization	Gain (dBi)
[8], 2019	41 × 100 × 1.6	0.88-0.96 / 2.28-2.57	LP	4.37
[9], 2020	85×85×1.6	0.882-0.936 / 2.35-2.58	CP	1.4 / 3.1
[10], 2021	104×104× 1.524	0.840-0.960 / 2.4-2.48	CP	0.8 / 4.6
[11], 2024	120×140× 0.817	0.881-0.942 / 2.32-2.52	CP	-1.26 / 3.26
Proposed antenna	104×104×1.524	0.866-1.05 / 2.25-3.13 / 3.48-3.8	CP/EP	1.73 / 5.7 / 5.9

3.6 Conclusion

In this chapter, we have designed a circularly polarized reader antenna for UHF/SHF applications with a size of $104 \times 104 \times 1.524\ mm^3$, covering three frequency bands at 0.915 GHz, 2.4 GHz and 3.7 GHz. The proposed design demonstrates excellent performance across both UHF and SHF frequency bands. Key points include:

- **Reflection Coefficient:** Very low return loss values, indicating excellent impedance matching and minimal reflection level:
  −30.87 dB at 0.915 GHz (UHF) and even lower values at SHF: −45 dB, −49.39 dB, and −27.38 dB at 2.4, 2.8, and 3.7 GHz, respectively.

- **Polarization:** Maintains circular polarization with axial ratio values:
  Around 1 dB in UHF and up to 3 dB in SHF, within acceptable limits for reliable performance in varying environments.

- **Realized Gain:**
  1.73 dBi at UHF and up to 5.9 dBi at SHF, indicating a strong radiation capability, especially at higher frequencies.

- **Total Efficiency:** Very high, reaching up to 98%, which means minimal power losses and excellent radiation efficiency.

- **Radiation Pattern:** Broadside bidirectional characteristics with significant gain at 0.915 and 2.4 GHz, supporting targeted communication applications.

In summary, the antenna is highly efficient, well-matched, and provides stable circular polarization radiation and strong performance across multiple frequency bands, making it a strong candidate for multi-band RFID and wireless communication systems.

Chapter 4

Design of a circularly polarized RFID tag antenna for UHF band use

Sommaire

4.1 Introduction

In this chapter, we discuss the design and the simulation of a miniaturized circularly polarized RFID tag antenna that operates at the UHF band of 915 MHz. We display the axial ratio, return loss, realized gain, efficiency, and radiation pattern of the proposed tag antenna. All results are obtained by using CST Studio Microwave Software. The tag antenna feeding is based on two 90 degree delays to make the antenna circularly polarized. Meander-lines are used in the miniaturization of the antenna. Our objective in this chapter is to design a miniaturized circularly polarized UHF tag antenna resonant at 915 MHz with enhanced gain and integration of a chip. After simulating the proposed design using CST software, we have obtained the results.

4.2 Tag antenna

4.2.1 Design process

In order to create the miniaturized and circularly polarized RFID tag antenna for the UHF band, we have to follow several steps and considerations. Figure 4.1 provides an overview of the design process.

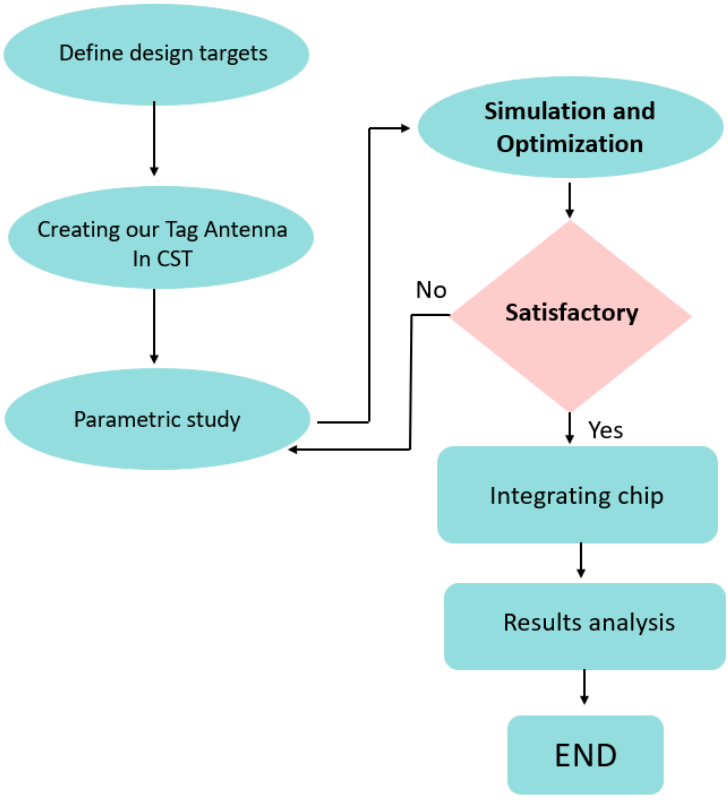

Figure 4.1: Methodology flowchart for antenna design process.

The following flowchart represents the main steps in obtaining the desired antenna. The first stage was to define the design target. Once the objectives are set, the antenna is created in CST Studio after the substrate and conductor materials are chosen. A parametric study is then conducted to analyze the effect of each parameter used. Then, the simulation and optimization; if the results are unsatisfactory, the process returns to the

previous step (parametric study). If the results are satisfactory, then we can integrate the chip to our antenna. Finally, a second round of simulation; however, the results analysis is added now to achieve high performance and to ensure that the entire system functions as intended, leading to the end of the design process.

4.2.2 Tag antenna design

The antenna development is carried out in two stages: the initial antenna design is based on the two 90° delays as in [67]. Then we have made modifications to achieve the final tag antenna design with the required performance.

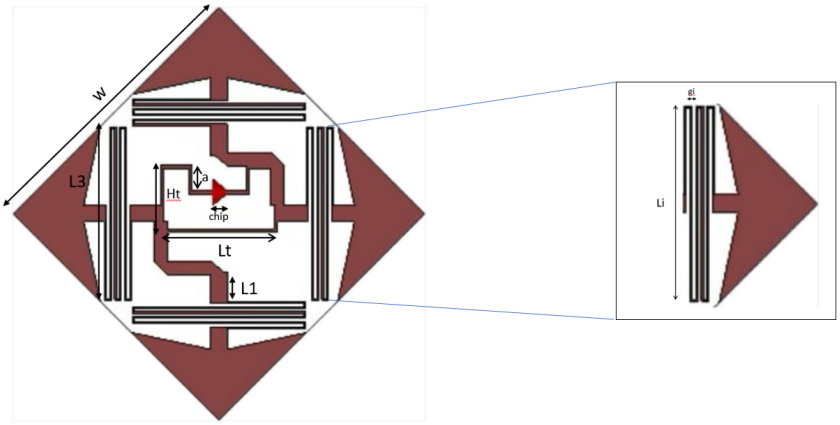

Figure 4.2: Geometry of the proposed tag antenna.

4.2.3 Tag antenna without chip

4.2.3.1 Input impedance

Figure 4.3 represents the input impedance of the proposed tag antenna in Ω as a function of frequency (MHz). The real and imaginary parts of the antenna input impedance are shown in this figure, where $Z_{ant} = 10 + j78\ \Omega$ at 915 MHz, which is similar to the UHF Gen2 STRAP chip, which has $10 - j64\ \Omega$ as impedance.

4.2.3.2 Axial ratio

Figure 4.4 illustrates the axial ratio (AR) in dB as a function of frequency in MHz for three different values of the design parameter denoted Li. The following results show that the configuration with Li = 20.75 mm and a = a0 = 3 mm achieves the lowest axial ratio at 915 MHz (AR< 3dB), indicating the presence of circular polarization.

Other parameters were used here in addition to Li to achieve the previous results; however, Li was the main parameter.

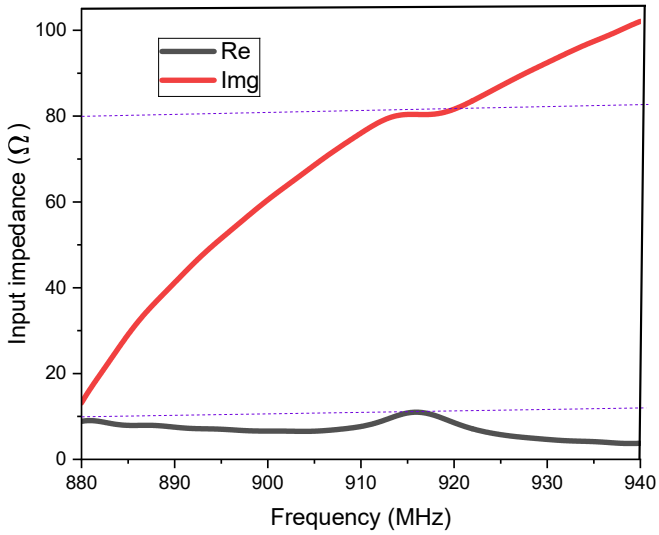

Figure 4.3: Input impedance of the proposed tag antenna as a function of frequency.

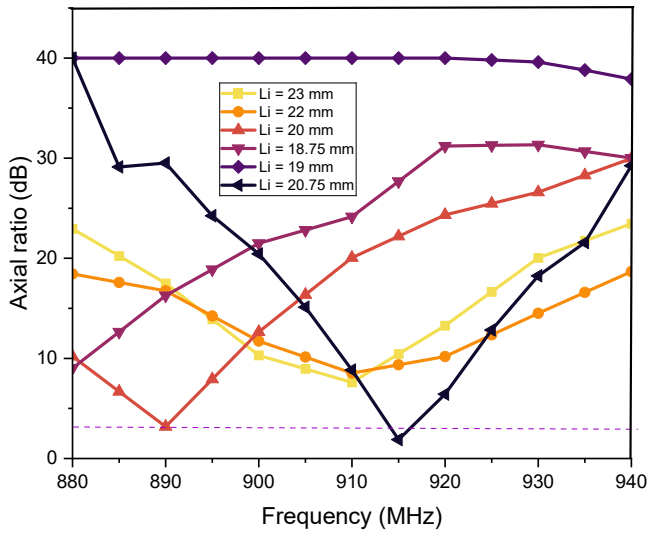

Figure 4.4: Axial ratio (dB) as a function of frequency of the proposed chipless tag antenna.

4.2.4 Tag antenna with chip

4.2.4.1 Reflection coefficient of the proposed tag antenna with chip

Figure 4.5 represents the line graphs for the first attempts used to obtain effective results of the magnitude of reflection coefficient $|S_{11}|$ as a function of frequency (MHz) of the proposed RFID tag antenna. Parameters denoted shiftT and $d1$ are crucial to enhance the S_{11}.

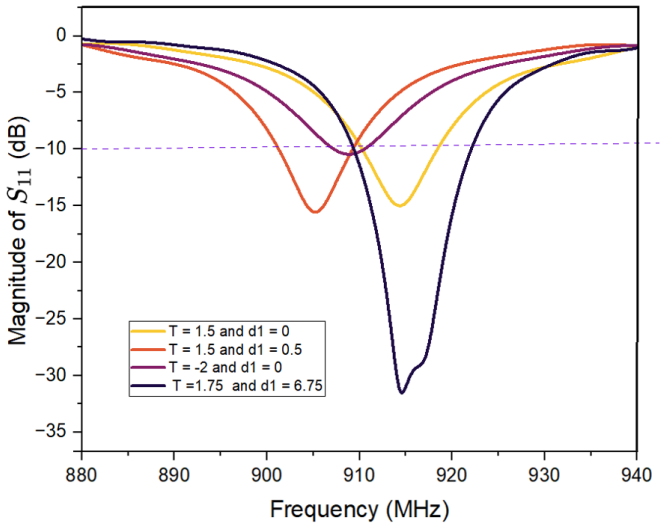

Figure 4.5: Magnitude of S_{11} as a function of frequency of the proposed tag antenna.

4.2.5 Finalized tag antenna design

The design of the new antenna, in Figure 4.2, retains some properties from the initial design (built on a square Rogers RO4003C substrate with a dielectric constant of 3.55 and a loss tangent of 0.0027). However, the dimensions have been modified to 35 × 35 × 0.508 mm^3. In addition, the shape of the four triangles was changed by introducing a slight curve to enhance the axial ratio for better circular polarization (CP). The meander lines remains the same, however, we altered the end circles to squares to reduce simulation time. Furthermore, delay elements are replaced by L-shaped delays with a slight curve, and the T-matched remained the same for better impedance matching. These modifications aim to shift the antenna back to the UHF band and improve the axial ratio to be lower than 3 dB to achieve circular polarization.

Table 4.1: Dimensions of the finalized antenna.

Parameter	W	chip	L_1	L_i	L_3	w_2	w_1	g_i	L_t	H_t	a	a_0
Value (mm)	35	0.5	3.6	20.75	21	1.6	0.4	0.4	14	8	3	3

4.2.6 RFID tag antenna with chip

In this section, results are presented using the Gen2 STRAP chip. The location of the chip and the port are at the antenna input as shown in figure 4.6.

To minimize power loss, it is essential to ensure proper impedance matching between the tag antenna and the chip. To achieve optimal power transfer and minimal reflection, the antenna impedance must be equal to the complex conjugate of the chip impedance.

$$Z_{ant} = Z^*_{chip} \tag{4.1}$$

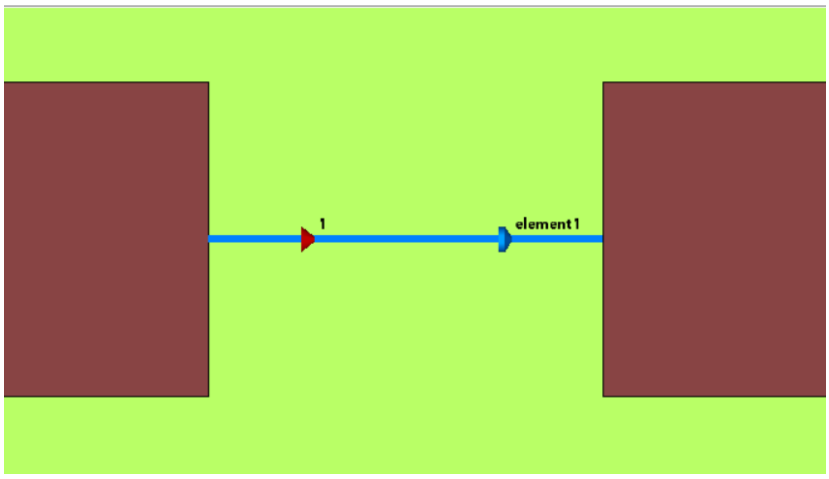

Figure 4.6: Location of the chip at the tag antenna input.

4.2.6.1 Reflection coefficient

Figure 4.7 represents the magnitude of the reflection coefficient $|S_{11}|$ as a function of frequency (MHz) of the proposed RFID tag antenna. The resonant frequency is at 915 MHz, while ($|S_{11}|$ < -10 dB) covers a wide bandwidth ranging from 909.47 MHz to 922.34 MHz, which supports robust performance in varying environments. The reflection coefficient at 915 MHz was about -31.12 dB, indicating a well-matched antenna.

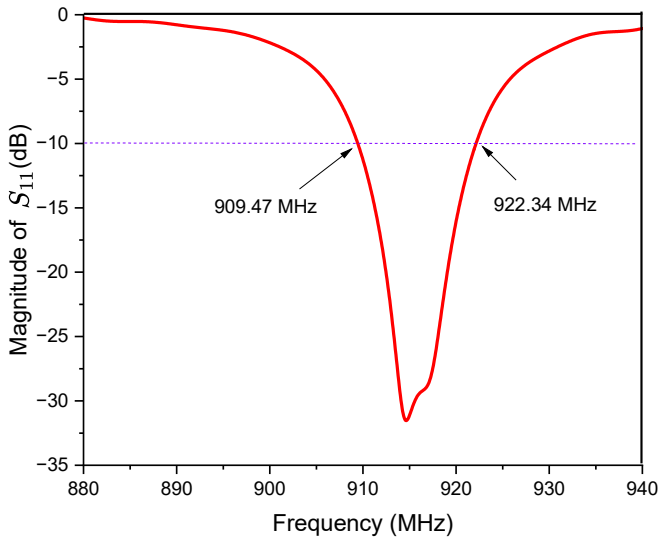

Figure 4.7: Magnitude of S_{11} in dB as a function of frequency in MHz of the proposed tag antenna.

4.2.6.2 Axial ratio

Figure 4.8 shows the value of the axial ratio in (dB) versus the frequency (MHz) of the proposed tag antenna. At the resonant frequency 915 MHz, the value of the axial ratio was (1.88 dB < 3 dB), and this indicates that the radiation of the RFID tag antenna is circular, and we achieved the circular polarization characteristics.

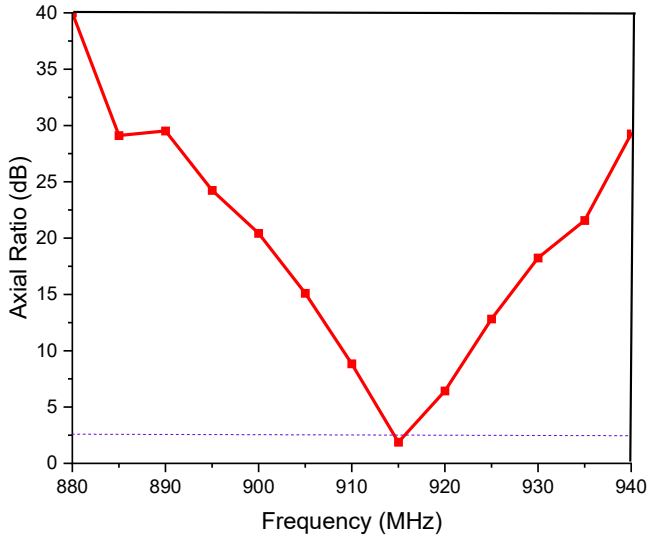

Figure 4.8: Axial ratio (dB) as a function of frequency of the proposed tag antenna.

4.2.6.3 Realized gain

Figure 4.9 displays the realized gain of the proposed antenna in (dB) as a function of the frequencies in (MHz). The peak of the realized gain at 915 MHz is 1.62 dBi, which indicates optimal power transmission efficiency, directly influencing the tag reading range.

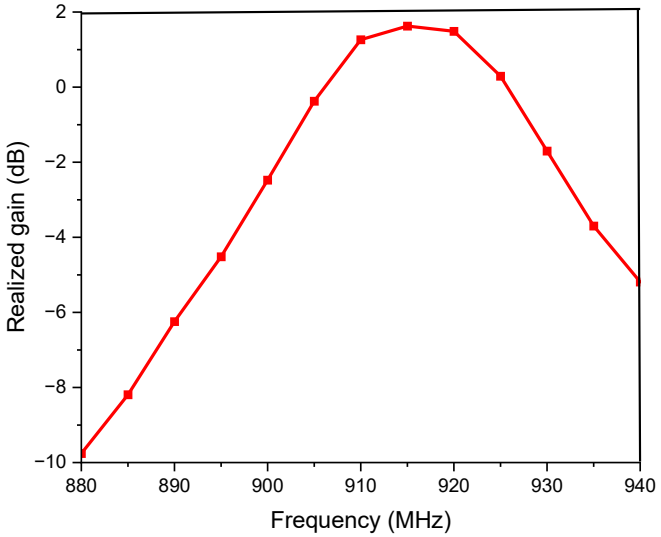

Figure 4.9: Realized gain (dB) as a function of frequency of the proposed tag antenna.

4.2.6.4 Total efficiency

Figure 4.10 shows the total radiation efficiency of the proposed tag antenna as a function of frequency. At 915 MHz, the efficiency reaches 96% ,which means that 96% of the

antenna input is converted into electromagnetic radiation. In addition, it illustrates the relation between the antenna gain and antenna efficiency as it is well explained in Chapter 2.

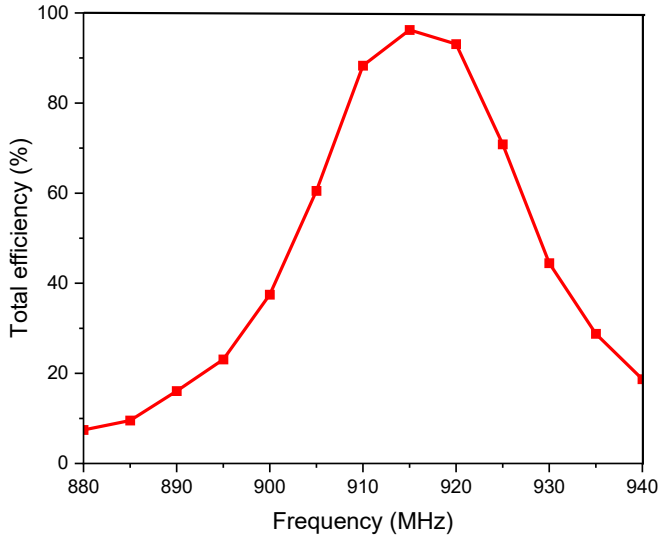

Figure 4.10: Efficiency in % as a function of frequency of the proposed tag antenna.

4.2.6.5 Radiation pattern

Figure 4.11 represents the radiation pattern of the proposed tag antenna at 915 MHz for different angular cuts in two different planes: φ = 0° and φ = 90° (the x-z and y-z planes). Figure 4.11a shows the radiation pattern for φ = 0° in polar representation of the proposed tag antenna with a maximum gain of 1.62 dBic. Figure 4.11b represents the radiation pattern for φ = 90° in polar representation of the proposed tag antenna with a maximum gain of 1.62 dBic. These figures show a maximum bidirectional radiation at frequency 915 MHz. Figure 4.12 represents the 3D radiation pattern of the proposed tag antenna at 915 MHz. It shows a broadband bidirectional radiation.

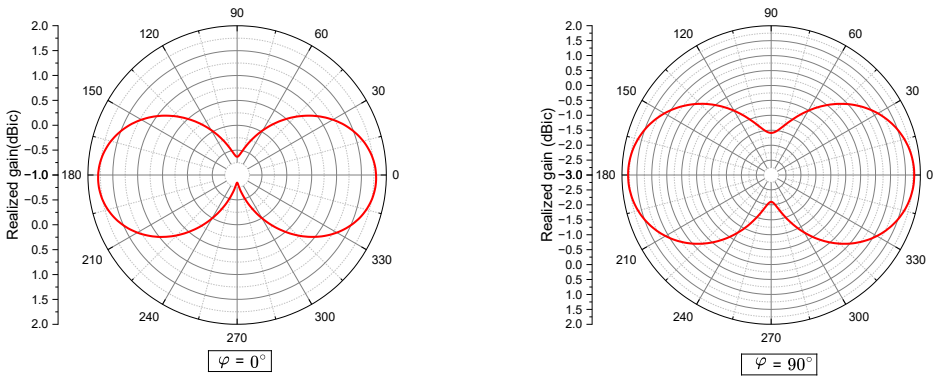

(a) φ = 0° (b) φ = 90°

Figure 4.11: Radiation pattern of the tag antenna at 915 MHz at φ = 0° and φ = 90°.

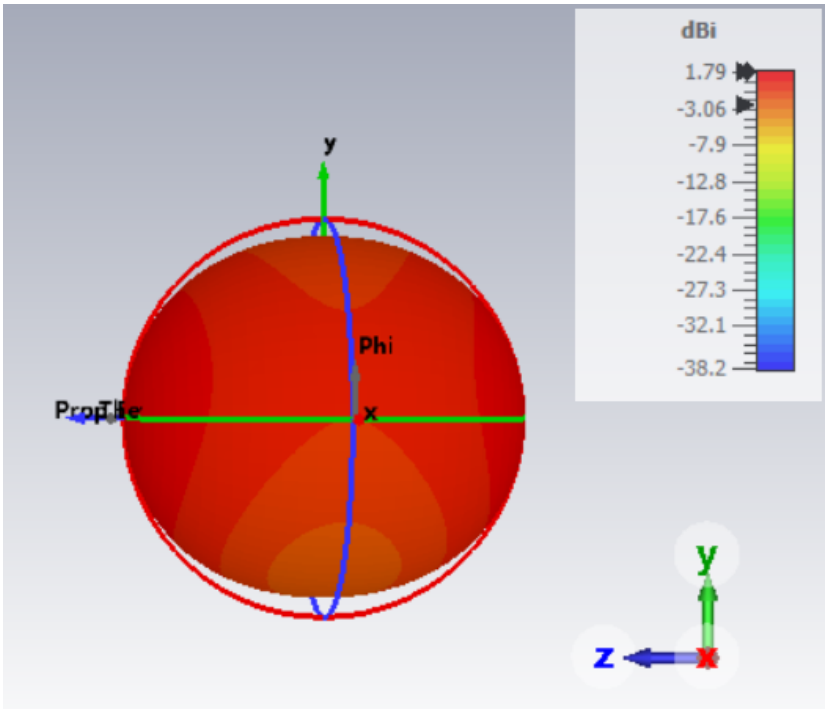

Figure 4.12: Radiation pattern of the proposed tag antenna at 915 MHz in 3D.

4.2.6.6 Electric field

Figure 4.13 shows the radiated electric field at various instances at 915 MHz, when $\omega t = 0°$ (fig. 4.13a), $\omega t = 90°$ (fig. 4.13b), $\omega t = 180°$ (fig. 4.13c), and $\omega t = 270°$ (fig. 4.13d). When the Z-direction is positive (z>0), the electric field is observed to spin counterclockwise, showing thereby a right-hand circular polarization (RHCP). When the Z-direction is negative (z<0), the electric field is observed to exhibit a left-hand circular polarization (LHCP).

Figure 4.14 represents the surface current of the tag antenna at 915 MHz for two instances ($\omega t = 0°$ and $\omega t = 90°$), where the substrate current goes to zero.

4.2.6.7 Maximum reading range of the RFID tag

In order to calculate the maximum reading range of the proposed RFID tag antenna, we use the following equation:

$$D_{max} = \frac{\lambda}{4\pi}\sqrt{\frac{EIRP \times G_r \times \tau}{P_{th}}} \tag{4.2}$$

where,

EIRP: Equivalent Isotropic Radiated Power.
G_r: Received gain of the antenna.
P_{th}: The sensitivity of the UHF Gen2 STRAP chip (in Watts).
τ: Transmission coefficient.
We now proceed with the numerical application of the above equation:

$$\lambda = \frac{c}{f} = \frac{3 \times 10^8}{915 \times 10^6} = 0.327 \text{ m}$$

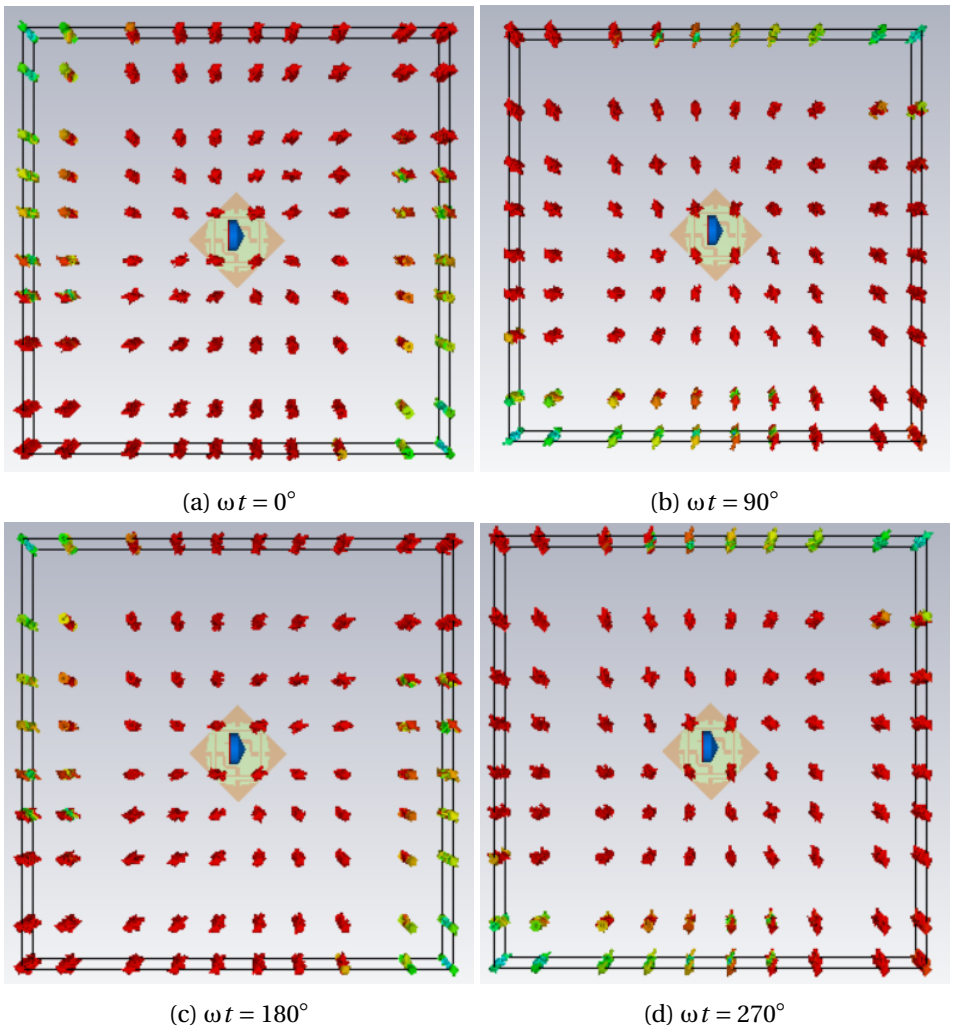

(a) $\omega t = 0°$ (b) $\omega t = 90°$

(c) $\omega t = 180°$ (d) $\omega t = 270°$

Figure 4.13: The behavior of the electric field of the proposed tag antenna at various instances at 915 MHz.

We have,

EIRP = 4 W;

$G_r = 1.62$ dBi $= 10^{1.62/10} \approx 1.45$;

$P_{th} = -13$ dBm $= 5.012 \times 10^{-5}$ W;

$\tau = 1$.

Then, we get the reading range of the proposed tag as follows:

$$D_{max} = \frac{0.327}{4\pi}\sqrt{\frac{4 \times 1.45 \times 1}{5.012 \times 10^{-5}}} \approx 8.84 \text{ m}$$

The calculated reading range is approximately 8.84 meters. This result shows how antenna gain and chip sensitivity affect the read distance. Small variations in these two parameters can significantly affect the range of the RFID tag antenna, making them critical in the performance of the RFID system.

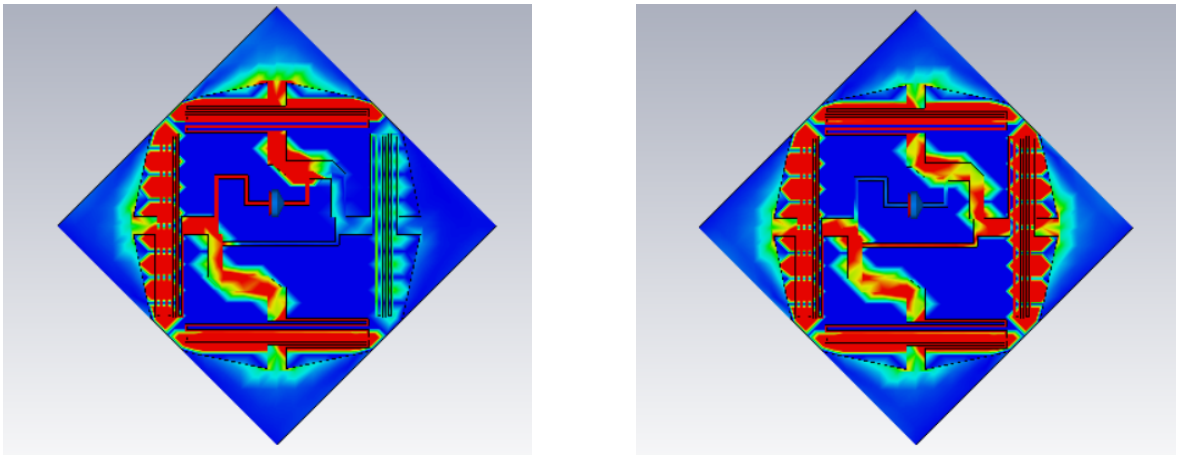

(a) $\omega t = 0°$ (b) $\omega t = 90°$

Figure 4.14: Surface current of the tag antenna at 915 MHz.

4.3 Performance comparisons with reported antennas

Table 4.2 illustrates a comparison of antenna performance characteristics among the proposed RFID tag antenna and five different previously published works in the literature, in terms of antenna size, frequency bandwidth, field polarization, gain, and reading range. The provided table shows that the proposed tag antenna has the smallest size of $35 \times 35 \times 0.508$ mm^3 compared to the antenna sizes in [3–7]. In terms of gain, the proposed tag antenna demonstrates competitive performance compared to works in [3–6], except the work in [7], which achieves 6 dBi of gain. However, it occupies a large surface of $220 \times 30 \times 1$ mm^3, as well as, the antenna does not show a circularly polarized radiation and only 5 meters of reading range is exposed. The proposed tag antenna shows the longer reading range of 8.84 m outperforming other antennas, which makes it highly suitable for long-range RFID applications. As well as, the proposed tag shows circularly polarized radiation in a broadside bidirectional radiation with a gain of 1.62 dBic. In summary, the proposed RFID tag antenna, offers a compact size, wide bandwidth, and long reading range compared to the existing previously published works in the literature. This makes it an excellent candidate for RFID applications dedicated to the UHF band in random mobility use.

Table 4.2: Comparison of antenna performance characteristics.

Ref., year	Size (mm^3)	Bandwidth (MHz)	Field Polarization	Gain (dBi)	Reading range (m)
[3], 2020	$\pi \times 36 \times 1.27$	902-944	CP	-30.4	0.8
[4], 2021	50×50×4.5	908-924	CP	-7.1	5.8
[5], 2022	55.2×44.2×1.5	920	LP	-4.11	8.14
[6], 2024	38×20×1.15	915	LP	-7.8	5.2
[7], 2024	220×30×1	902–928	LP	6	3-5
Proposed antenna	35×35×0.508	909.47-922.34	CP	1.62	8.84

4.4 Conclusion

In this chapter, we have designed a miniaturized tag antenna with circularly polarized radiation. The proposed tag radiates bidirectionally with a gain of 1.62 dBic in stable radiation. The low size of the antenna of $35 \times 35 \times 0.508$ mm^3 makes it very compact, ideal for space-constrained applications. At the resonant frequency 915 MHz, the antenna achieves a low reflection coefficient of –31.12 dB, indicating excellent impedance matching. In addition, the tag offers a large read range of 8.84 meters, which makes it suitable for long-range RFID applications. Compared to other previously published works in the literature, the proposed design demonstrates superior performance in terms of size and reading range, making it practical for modern RFID systems.

General Conclusion

To sum up, this project aims to design a miniaturized circularly polarized tag antenna for the UHF American band of 915 MHz. Also, a dual-band circularly-polarized reader antenna, which operates at both 915 MHz and 2.45 GHz, has been designed for RFID applications. Both of the proposed antennas have been designed to achieve characteristics meeting market requirements. The CST software tool is used to design, simulate and analyze the results.

In the first chapter, we have presented the RFID systems by outlining its concepts, components, and various classifications. Furthermore, we have explained how it operates, several standards, regulations, and its applications. We have concluded the chapter with the benefits and limits of RFID systems.

Then, in the second chapter, we have shown the main characteristics of antennas, such as radiation parameters and electrical parameters. In addition, different methods of matching and wandering have been demonstrated. Moreover, we have reviewed the patch antenna configuration and its various feeding techniques.

The third chapter has focused on designing a dual-band circularly-polarized (CP) reader antenna that operates at 915 MHz and 2.45 GHz radio frequency identification (RFID) bands. This is based on the use of the sequential phase technique exciting with phases of 0°, 90°, 180°, and 270°. Simulation results have been obtained using the CST Studio Microwave simulation tool. The dimensions of the proposed reader antenna are 104 × 104 × 1.524 mm^3. We have obtained very low return loss values, indicating excellent impedance matching, with -30.87 dB at 915 MHz (UHF) and even lower values at SHF of -45 dB, -49.39 dB, and -27.38 dB at 2.4, 2.8, and 3.7 GHz, respectively. An axial ratio around 1 dB in UHF and up to 3 dB in SHF has been achieved within acceptable limits for reliable performance in varying environments. Moreover, a realized gain of 1.73 dBi at UHF and up to 5.9 dBi at SHF, is obtained, with a very high total efficiency reaching 98%. Broadband bidirectional radiation characteristics have been achieved with significant gains at 915 MHz and 2.4 GHz, supporting targeted communication applications.

In the fourth chapter, a miniaturized tag antenna with circularly polarized radiation has been designed. The proposed tag radiates bidirectionally with a gain of 1.62 dBic in stable radiation, with a total efficiency of 96%. This means that 96% of the antenna input energy is converted into electromagnetic waves. The low size of the antenna of 35 × 35 × 0.508 mm^3 makes it very compact, ideal for space-constrained applications. At the resonant frequency 915 MHz, the antenna achieves a very low reflection coefficient of –31.12 dB, indicating excellent impedance matching with a minimal reflection level. Furthermore, at 915 MHz the value of the axial ratio is 1.88 dB, which indicates that the radiation of the RFID tag antenna is circularly polarized. The results have been presented by using the Gen2 STRAP chip having an impedance of 10-j64 Ω. The tag offers a large read range up to 8.84 meters, which makes it suitable for long-range RFID applications. Compared to other previously published works in the literature, the proposed design demonstrates superior performance in terms of size and reading range, as well as the polarization matching, making it practical for modern RFID systems.

Bibliography

[1] S. A. Weis, "Rfid (radio frequency identification): Principles and applications," *System*, vol. 2, no. 3, pp. 1–23, 2007.

[2] S. Sharma, M. R. Tripathy, and A. K. Sharma, "Fss supported longer read range passive uhf rfid reader antenna," in *2021 IEEE International Conference on RFID Technology and Applications (RFID-TA)*, pp. 207–210, IEEE, 2021.

[3] Y. Zhang, C. Liu, X. Liu, and K. Zhang, "A miniaturized circularly polarized implantable rfid antenna for biomedical applications," *International Journal of RF and Microwave Computer-Aided Engineering*, vol. 30, no. 3, p. e22105, 2020.

[4] D. Le, S. Ahmed, L. Ukkonen, and T. Björninen, "A small all-corners-truncated circularly polarized microstrip patch antenna on textile substrate for wearable passive uhf rfid tags," *IEEE Journal of Radio Frequency Identification*, vol. 5, no. 2, pp. 106–112, 2021.

[5] F. Erman, D. Mansour, M. Kouali, A. Shabaneh, L. Leifsson, S. Koziel, E.-H. Lim, and E. Hanafi, "Low-profile interdigitated uhf rfid tag antenna for metallic objects," *IEEE Access*, vol. 10, pp. 90915–90923, 2022.

[6] J. Wang and J. Yuan, "A low-profile uhf rfid tag antenna loaded with rectangular loop for double-sided anti-metal applications.," *Progress in Electromagnetics Research C*, vol. 141, 2024.

[7] S. López-Soriano, J. Melià-Seguí, and J. P. Granados, "Uhf rfid wristbands: A long-range, durable, flexible, and low-cost tag antenna design," *IEEE Journal of Radio Frequency Identification*, vol. 8, pp. 125–133, 2024.

[8] A. Romputtal and C. Phongcharoenpanich, "Iot-linked integrated nfc and dual band uhf/2.45 ghz rfid reader antenna scheme," *IEEE Access*, vol. 7, pp. 177832–177843, 2019.

[9] F.-P. Lai, J.-F. Yang, and Y.-S. Chen, "Compact dual-band circularly polarized antenna using double cross dipoles for rfid handheld readers," *IEEE Antennas and Wireless Propagation Letters*, vol. 19, no. 8, pp. 1429–1433, 2020.

[10] R. Xu, J. Liu, K. Wei, W. Hu, Z.-J. Xing, J.-Y. Li, and S. S. Gao, "Dual-band circularly polarized antenna with two pairs of crossed-dipoles for rfid reader," *IEEE Transactions on Antennas and Propagation*, vol. 69, no. 12, pp. 8194–8203, 2021.

[11] B. Mekimah, L. Manel, and K. Khoula, *FSS reflector-based RFID reader antenna for UHF/SHF applications.* University Kasdi Merbah Ouargla, 2024.

[12] F. Chetouane, "An overview on rfid technology instruction and application," *IFAC-PapersOnLine*, vol. 48, no. 3, pp. 382–387, 2015.

[13] A. Hamidi, B. Mekimah, S. Berhab, T. Djerafi, A. Belhedri, and M. Boulesbaa, "A high gain circularly polarized passive rfid tag on a metallic reflector for uhf band applications," in *2024 8th International Conference on Image and Signal Processing and their Applications (ISPA)*, pp. 1–4, IEEE, 2024.

[14] S. Preradovic and N. C. Karmakar, "Rfid readers-a review," in *2006 International Conference on Electrical and Computer Engineering*, pp. 100–103, IEEE, 2006.

[15] M. A. Baballe, "A study on the components used in rfid system and its challenges," *Global J Res Eng Comput Sci*, vol. 1, no. 1, pp. 21–27, 2021.

[16] K. Finkenzeller, *RFID handbook: fundamentals and applications in contactless smart cards, radio frequency identification and near-field communication*. John wiley & sons, 2010.

[17] M. Bouet and A. L. Dos Santos, "Rfid tags: Positioning principles and localization techniques," in *2008 1st IFIP Wireless Days*, pp. 1–5, Ieee, 2008.

[18] P. Brun-Murol, *Vers une méthodologie normalisée d'évaluation des solutions RFID en application de sécurité*. PhD thesis, École Polytechnique de Montréal, 2013.

[19] S. M. Chiang, *Design And Optimization Of Compact On-Metal Ultra High Frequency RFID Tag Antennas*. PhD thesis, UTAR, 2021.

[20] U. RFID, "Les systèmes rfid uhf passifs et leur environnement," 2009.

[21] Y. Zhang, M. G. Amin, and S. Kaushik, "Localization and tracking of passive rfid tags based on direction estimation," *International Journal of Antennas and Propagation*, vol. 2007, no. 1, p. 017426, 2007.

[22] Y. J. Patel, "Future scope of rfid technology and advantages & applications," *International Journal of Scientific Research in Science and Technology*, vol. 3, no. 8, pp. 542–548, 2017.

[23] R. Bhochhibhoya, *Mobile tag reading in a multi-reader RFID environment*. Oklahoma State University, 2008.

[24] R. Kheddam, *Approches logicielles de sûreté de fonctionnement pour les systèmes RFID*. PhD thesis, Université de Grenoble, 2014.

[25] J. Waldrop, D. W. Engels, and S. E. Sarma, "Colorwave: an anticollision algorithm for the reader collision problem," in *IEEE International Conference on Communications, 2003. ICC'03.*, vol. 2, pp. 1206–1210, IEEE, 2003.

[26] D. W. Engels and S. E. Sarma, "The reader collision problem," in *IEEE international conference on systems, man and cybernetics*, vol. 3, pp. 6–pp, IEEE, 2002.

[27] J. Ho, D. W. Engels, and S. E. Sarma, "Hiq: a hierarchical q-learning algorithm to solve the reader collision problem," in *International Symposium on Applications and the Internet Workshops (SAINTW'06)*, pp. 4–pp, IEEE, 2006.

[28] S. M. Birari and S. Iyer, "Mitigating the reader collision problem in rfid networks with mobile readers," in *2005 13th IEEE International Conference on Networks Jointly held with the 2005 IEEE 7th Malaysia International Conf on Communic*, vol. 1, pp. 6–pp, IEEE, 2005.

[29] G. Khadka and S.-S. Hwang, "Tag-to-tag interference suppression technique based on time division for rfid," *Sensors*, vol. 17, no. 1, p. 78, 2017.

[30] S.-Y. Kim, H.-K. Park, J.-K. Lee, Y.-C. Ra, and S.-W. Lee, "A study on control method to reduce collisions and interferences between multiple rfid readers and rfid tag," in *2009 International Conference on New Trends in Information and Service Science*, pp. 339–343, IEEE, 2009.

[31] B. Mekimah, K. Serraye, and M. Gouarah, *Design of a circularly polarized RFID tag antenna based on FSS reflector for UHF applications*. University Kasdi Merbah Ouargla, 2024.

[32] B. Mekimah, M. M. Naami, and N. Hafiane, *Conception et simulation d'une antenne tag RFID passive à polarisation circulaire dédiée aux applications UHF*. University Kasdi Merbah Ouargla, 2023.

[33] C. R. Medeiros, J. R. Costa, and C. A. Fernandes, "Rfid reader antennas for tag detection in self-confined volumes at uhf," *IEEE Antennas and Propagation Magazine*, vol. 53, no. 2, pp. 39–50, 2011.

[34] D. Paret, *RFID at ultra and super high frequencies: theory and application*. John Wiley & Sons, 2009.

[35] A. Lazaro, D. Girbau, and D. Salinas, "Radio link budgets for uhf rfid on multipath environments," *IEEE transactions on antennas and propagation*, vol. 57, no. 4, pp. 1241–1251, 2009.

[36] P. Kumar, H. Reinitz, J. Simunovic, K. Sandeep, and P. Franzon, "Overview of rfid technology and its applications in the food industry," *Journal of food science*, vol. 74, no. 8, pp. R101–R106, 2009.

[37] K. Ahsan, H. Shah, and P. Kingston, "Rfid applications: An introductory and exploratory study," *arXiv preprint arXiv:1002.1179*, 2010.

[38] H. Doğan, "Rfid applications in animal identification and tracking," *New Frontiers in Engineering*, pp. 66–93, 2023.

[39] N. K. Singh and P. Mahajan, "Application of rfid technology in libraries," *International Journal of Library and Information Studies*, vol. 4, no. 2, pp. 1–9, 2014.

[40] S. Abdoli, "Rfid application in municipal solid waste management system," 2009.

[41] K. S. Rao, P. V. Nikitin, and S. F. Lam, "Impedance matching concepts in rfid transponder design," in *Fourth IEEE Workshop on Automatic Identification Advanced Technologies (AutoID'05)*, pp. 39–42, IEEE, 2005.

[42] G. A. Vera, Y. Duroc, and S. Tedjini, "Spectre du signal de backscattering des tags rfid uhf passifs," in *Journées Nationales Microondes*, 2013.

[43] B. Mekimah, T. Djerafi, A. Messai, A. Belhedri, M. Boulesbaa, and A. Hamidi, "Circularly polarized square loop shaped passive rfid transponder for thin uhf applications in random mobility use," in *2023 Workshop on Microwave Theory and Technology in Wireless Communications (MTTW)*, pp. 144–148, IEEE, 2023.

[44] B. Glover and H. Bhatt, *RFID essentials*. " O'Reilly Media, Inc.", 2006.

[45] D. Arnaud-Cormos, T. Letertre, A. Diet, and A. Azoulay, "Influence des ondes électromagnétiques sur les performances rfid," in *19e Colloque Internationale Optique Hertzienne & Diélectriques (OHD 2007)*, pp. cd–rom, 2007.

[46] D. Masse, "Rfid handbook: Fundamentals and applications in contactless smart cards and identification second edition.," *Microwave Journal*, vol. 47, no. 10, pp. 168–169, 2004.

[47] D. M. Dobkin and S. M. Weigand, "Environmental effects on rfid tag antennas," in *IEEE MTT-S International Microwave Symposium Digest, 2005.*, pp. 135–138, IEEE, 2005.

[48] A. Ghiotto, S. Cantalice, T.-P. Vuong, A. Pouzin, G. Fontgalland, and S. Tedjini, "Miniaturized patch antenna for the radio frequency identification of metallic objects," in *2008 IEEE MTT-S International Microwave Symposium Digest*, pp. 583–586, IEEE, 2008.

[49] M. Kaur, M. Sandhu, N. Mohan, and P. S. Sandhu, "Rfid technology principles, advantages, limitations & its applications," *International Journal of Computer and Electrical Engineering*, vol. 3, no. 1, pp. 151–157, 2011.

[50] O. Picon, L. Cirio, C. Ripoll, G. Baudoin, J.-F. Bercher, and M. Villegas, *Les antennes: Théorie, conception et applications*. Dunod, 2009.

[51] B. Mekimah, A. Messai, and T. Djerafi, *Amélioration des caractéristiques des patchs microbandes pour les applications ultra large bande*. PhD thesis, Université Frères Mentouri-Constantine 1, 2020.

[52] S. A. Ahson and M. Ilyas, *RFID handbook: applications, technology, security, and privacy*. CRC press, 2017.

[53] S. Liu and K. Yu, "Successive multivariate variational mode decomposition," *Multidimensional Systems and Signal Processing*, vol. 33, no. 3, pp. 917–943, 2022.

[54] B. Mekimah, A. Messai, and A. Belhedri, "Gain enhancement of a cpw-fed dipole antenna using a novel multiband planar artificial magnetic conductor surface for uwb applications," *International Journal of Wireless and Mobile Computing*, vol. 21, no. 2, pp. 141–152, 2021.

[55] B. Mekimah, T. Djerafi, A. Messai, and A. Belhedri, "A reconfigurable antenna in frequency band and radiation using active frequency selective surfaces on the basis of pin diodes," in *2021 IEEE Microwave Theory and Techniques in Wireless Communications (MTTW)*, pp. 238–242, IEEE, 2021.

[56] B. Mekimah, A. Messai, and A. Belhedri, "Analysis of the effect of dielectric losses on the bandwidth of microstrip patch antenna in stacked geometry and modelling," *SN Applied Sciences*, vol. 2, no. 4, p. 767, 2020.

[57] L. Boccia and O. Breinbjerg, "Antenna basics," *Space Antenna Handbook*, pp. 1–35, 2012.

[58] B. Mekimah, T. Djerafi, A. Messai, and A. Belhedri, "Broadband circularly polarized cpw-fed asymmetrically-shaped slot patch antenna for x band applications," *Progress In Electromagnetics Research Letters*, vol. 91, pp. 137–143, 2020.

[59] B. Mekimah, M. Abderraouf, M. A. Meriche, and A. Belhedri, "Miniaturized and circularly polarized inverted c shaped patch antenna for x and ku bands applications," in *2018 18th Mediterranean Microwave Symposium (MMS)*, pp. 361–364, IEEE, 2018.

[60] C. A. Balanis, *Antenna theory: analysis and design*. John wiley & sons, 2016.

[61] I. Singh, V. Tripathi, *et al.*, "Micro strip patch antenna and its applications: a survey," *Int. J. Comp. Tech. Appl*, vol. 2, no. 5, pp. 1595–1599, 2011.

[62] A. R. O. Mumin Warfaa, *Analysis of three different dielectric substrates on square ring microstrip antenna for wireless application*. PhD thesis, Universiti Tun Hussein Onn Malaysia, 2015.

[63] B. Mekimah, T. Djerafi, A. Messai, and A. Belhedri, "A reconfigurable multi-band antenna with a high selectivity in frequency on the basis of pin diodes," in *2022 19th International Multi-Conference on Systems, Signals & Devices (SSD)*, pp. 2074–2077, IEEE, 2022.

[64] O. P. E. Coll *et al.*, "les antennes: théorie, conception et application," *Préface de Maurice Bellanger*, 2009.

[65] G. Marrocco, "The art of uhf rfid antenna design: Impedance-matching and size-reduction techniques," *IEEE antennas and propagation magazine*, vol. 50, no. 1, pp. 66–79, 2008.

[66] M. Alibakhshikenari, B. S. Virdee, P. Shukla, Y. Wang, L. Azpilicueta, M. Naser-Moghadasi, C. H. See, I. Elfergani, C. Zebiri, R. A. Abd-Alhameed, *et al.*, "Impedance bandwidth improvement of a planar antenna based on metamaterial-inspired t-matching network," *IEEE Access*, vol. 9, pp. 67916–67927, 2021.

[67] H. H. Tran, S. X. Ta, and I. Park, "A compact circularly polarized crossed-dipole antenna for an rfid tag," *IEEE Antennas and Wireless Propagation Letters*, vol. 14, pp. 674–677, 2014.